MASTER THESIS

TITLE: Thermal analysis of the state of charge of batteries

MASTER DEGREE: Master in Science in Telecommunication Engineering & Management

AUTHOR: Victòria Júlia Ovejas Benedicto

DIRECTOR: Àngel Cuadras

DATE: 15th of November of 2010

Títol: Anàlisi tèrmic de l'estat de càrrega de les bateries

Autor: Victòria Júlia Ovejas Benedicto

Director: Àngel Cuadras

Data: 15 de novembre de 2010

Resum

És evident el creixent ús de dispositius elèctrics portàtils i autònoms (telèfons mòbils, portàtils, cotxes elèctrics, xarxes de sensors...). Aquests dispositius utilitzen les bateries com a font d'energia. Per tant, cada cop és més important de tenir un bon coneixement de l'energia restant a la bateria, per conèixer exactament en quin moment s'haurà de recarregar, així com de conèixer el seu estat d'envelliment per tal de saber quan caldrà canviar-la.

Les bateries de Li-ió han aportat molts avantatges respecte les seves predecessores. Proporcionen un voltatge més elevat, són més lleugeres i la densitat d'energia respecte el seu pes i volum és molt més gran.

En aquest projecte es proposa estimar la càrrega real restant a les bateries mitjançant les variacions de temperatura que es produeixen al seu interior tant durant la càrrega com durant la descàrrega. Es pretén trobar una solució senzilla, econòmica i que no requereixi elements externs. És per això que les mesures de temperatura es fan aprofitant un termistor que ja ve incorporat a les bateries de liti, la finalitat del qual és d'evitar sobreescalfaments.

S'ha fet servir una bateria de Li-ió amb una capacitat de 740mAh proporcionada per Varta Microbattery. A partir de mesures de corrent, tensió i temperatura, s'han calculat la resistència interna, el flux de calor dins la bateria i la impedància tèrmica. S'ha comprovat que és possible relacionar les variacions de temperatura, el corrent i la tensió amb la calor generada a la bateria i, a partir d'això, estimar-ne l'estat de càrrega (SoC).

També s'han fet cicles consecutius de càrrega i descàrrega i s'ha calculat la càrrega injectada i extreta per cadascun d'ells. Després, això s'ha relacionat amb l'estat de salut de la bateria (SoH). En aquest sentit ha calgut redefinir les expressions del SoC i SoH.

Title: Thermal analysis of the state of charge of batteries

Author: Victòria Júlia Ovejas Benedicto

Director: Àngel Cuadras

Date: 15th of November of 2010

Overview

Clearly there is nowadays an increasing use of portable electric devices (mobile phones, laptops, electric cars, sensor networks ...). These devices use batteries as a power source. Therefore, it is increasingly important to have a good knowledge of the remaining battery power, to exactly know at what point should be recharged. Moreover its wear out must also be known in order to replace it when necessary.

Li-ion batteries have provided many advantages over their predecessors. They provide a higher voltage, they are lighter and the energy density with respect to their weight and volume is much higher.

This project aims to estimate the actual remaining battery charge through temperature variations that occur inside the battery both during charging and discharging. The aim is to find a simple and cheap solution, which does not require external elements. For this reason, temperature measurements are carried out using a thermistor that is already present in lithium batteries. At present, its purpose is to avoid overheating.

A Li-ion battery with 740mAh capacity provided by VARTA Microbattery was used. From measurements of current, voltage and temperature we calculated the internal resistance, the heat flow inside the battery and the thermal impedance. It has been shown that it is possible to relate temperature variations, current and voltage to the heat generated in the battery. Thus, it is possible to estimate the state of charge of the battery (SoC) from temperature fluctuations.

In addition, consecutive charge and discharge cycles were carried out. Injected and extracted charge was calculated for each of them. Then, it was related to SoH. Finally, new definitions of SoC and SoH which consider their relationships are proposed.

A totes les persones que m'han fet costat i han cregut en mi durant tots aquests anys de carrera. Especialment als meus pares i al director de la tesi, Àngel Cuadras. Gràcies per la vostra paciència.

INDEX

INDEX OF FIGURES

INDEX OF TABLES

INTRODUCTION

As the use of devices powered by batteries is growing, it is increasingly important to know when to recharge or change a battery. For example, an electric car cannot be driven either without knowing how many miles you can do before having to recharge the battery; or a UAV (Unmanned Aerial Vehicle) cannot fly without the certainty of knowing how much will last the battery. Many examples like these can be found. It is also important because if the actual state of the battery is not accurately known these are replaced by new batteries probably long before they have completed their useful life. This waste of batteries could be saved if their State of Charge (SoC) and State of Health (SoH) were estimated. SoC represents the remaining energy in the battery and SoH describes the losses in capacity of the battery produced by aging.

Many investigations about SoC and SoH estimation have been carried out, based on voltage measurements, charge integration and resistance calculations. Unfortunately, none of these methods has been able to give an exact and accurate determination of battery parameters. Because of this we propose an approach based on thermal dissipation.

Our aim in this contribution is to relate temperature variations inside the battery due to heat dissipation during charge and discharge cycles with SoC and SoH. Nowadays, there are some attempts to relate the temperature and heat generated in the battery to the SoC and the SoH [1] [2] [3]. So far, it was studied how these parameters are related but heat generated in the battery was always measured by non-portable equipment. Lithium-based batteries include a thermistor in their package and we purpose to use it to overcome the portability problem. Currently, it is used only as a temperature control while charging or discharging the battery: if the upper temperature threshold is reached, the battery is disconnected. We aim at take advantage of this thermistor, not only using it as a protection element but also to monitor SoC and SoH, leading to a low energy consumption solution and low cost.

Mobile phones, laptop computers, cameras, electric cars or UAV are some examples of devices powered by lithium-based batteries. Lithium ion batteries are lighter than other technologies and have a higher density with respect to their weight and volume. Furthermore, with a single cell, the same voltage obtained by several cells of other technologies connected in series is achieved.

This work is divided in five chapters. The first one describes the theoretical foundations of batteries, the state of the art of battery monitoring and their main features and parameters. The second chapter specifies the particular batteries involved in the project and the methods used to carry out the measurements. Third chapter shows main results, which include voltage, current and temperature measurements. These results are discussed in chapter four. And, finally, chapter five summarizes the most relevant conclusions inferred from the project.

CHAPTER 1. BATTERIES DESCRIPTION

In this chapter, it will be explained what a battery is and its main features. Also heat effects present in batteries will be described and defined. A brief description over different chemistries will be done on the last part of that section.

A battery is an electrochemical cell or a combination of them and it is used to store energy. Batteries can be classified into primary batteries and secondary batteries. Primary batteries transform chemical energy into electrical energy only once while secondary batteries can do it more than one time. In other words, secondary batteries are rechargeable. The main difference between them is that the second ones are based on a reversible chemical reaction while the first ones are not [4].

1.1. The electrochemical cell and the cell reaction

Cell reaction is a chemical reaction that characterizes the battery. During discharge chemical compounds of higher energy are transformed into chemical compounds of lower energy through redox reactions and freeing electrons. A battery has two electrodes: one that absorbs electrons and one that releases electrons, thus the energy generated in that reaction causes an electric current flow.

Two electrodes, one negative and one positive (in secondary batteries, it depends on charge or discharge which of the two electrodes is the anode or cathode [4]), are immersed in an electrolyte as shown in Fig. 1.1. The reacting substances are usually stored within the electrodes but sometimes (depending on the battery type) they are also stored in the electrolyte. Often the electrolyte is only the medium for electrode reactions and ionic conductivity and does not appear on the cell reaction.

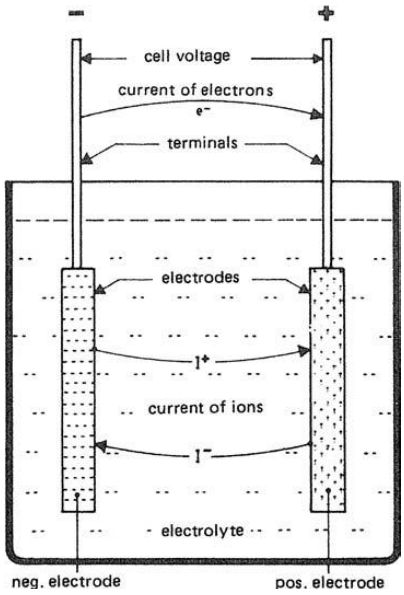

Fig. 1.1. Physical model of the battery

1.2. Battery parameters

Main parameters as are capacity, energy, current, SoC, SoH, voltage, resistance and self-discharge will be described in this section.

1.2.1. Capacity and energy

The capacity of a battery is defined by international convention as the electrical charge (in units of Ah) that can be drawn from the battery at a current *I(t)* (1.1).

$$C_{Ah} = \int_0^t I(t) \cdot dt \tag{1.1}$$

There are many factors that affect capacity: its design, the discharge current, the cut-off voltage, the temperature and the history of the battery. That is, the available charge is strongly servable on these parameters.

Nominal capacity (C_r) is the standard value provided by the manufacturer that characterizes the battery. It is usually specified for a constant current discharge at a certain temperature.

The energy that can be drawn from a battery can be calculated from the integration of the voltage multiplied by the discharge current (1.2).

$$E = \int_0^t V(t) \cdot I(t) dt \tag{1.2}$$

1.2.1.1 *Charge/discharge currents*

In the field of batteries, current (*I*) is represented as a multiple or fraction of the nominal capacity (1.3). For example, a battery is being charged or discharged at 1C means that it is charged or discharged at those Cr amperes (nominal capacity of the battery in Ah but expressed in A) during an hour. If it is done at 0.5C it will be charged or discharged during two hours at half C_r amperes.

$$I = m \cdot C_r \tag{1.3}$$

Where, *m* is a number that represents the multiple or fraction of the nominal capacity and C_r is the nominal capacity in Ah, but expressed in A.

1.2.2. State of charge and state of health

Two critical parameters for this project are State of Charge (SoC) and State of Health (SoH).

SoC describes the available fraction of energy with respect to the full capacity of the battery [5]. Equation (1.4) relates extracted charge with respect to nominal capacity of the battery while equation (1.5) represents inserted charge on the battery when charging it and compares it with nominal capacity. It is usually given as a percentage, being 100 % fully charged and 0 % discharged.

$$\mathrm{SoC} = \frac{\mathrm{C_r} - \int_0^t \mathrm{I} \cdot \mathrm{dt}}{\mathrm{C_r}} \tag{1.4}$$

$$\mathrm{SoC} = \frac{\int_0^t \mathrm{I} \cdot \mathrm{dt}}{\mathrm{C_r}} \tag{1.5}$$

SoH represents the aging of the battery and its current capacity. An imaginary division could be made in a battery: one section that represents the available energy, another one that is empty and can be fulfil and the last one that has no possibility to be reused (Fig. 1.2). This third section grows with the aging and usage of the battery and it is represented by SoH. Therefore, it means that battery capacity decreases with cycles. No formula was found in literature to calculate it. Then, any parameter that changes with cycles could be used for that purpose after a previous calibration.

Fig. 1.2. Three imaginary sections of a battery consisting of available energy, empty zone and unusable zone [6]

1.2.3. Voltage

By definition, the open-circuit voltage (V_{OC}) is the battery voltage under the equilibrium conditions, that is, the voltage when no current is flowing in or out of the battery and hence no reactions occur inside the battery [7]. It depends on temperature, SoC and SoH. After a current has flown through the battery, V_{OC} takes some time to be stabilized due to active material's diffusion [1]. This relaxation time depends basically on the charge rate that is being used.

The cell voltage under load (V_{cell}) depends on current, SoC and cell's history, like its lifetime or storage period. Typical V_{cell} curves while discharging a Li-ion battery with two different constant currents are shown in Fig. 1.3.

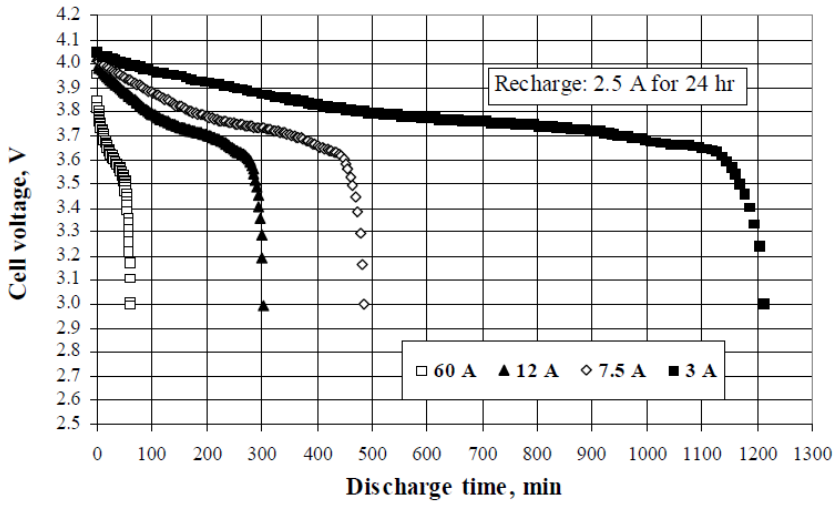

Fig. 1.3. Typical low-rate and high-rate discharges (at constant current) curves of a Li-ion battery [8]

In addition, typical cell voltages while discharging batteries composed by different chemistries are shown in Fig. 1.4. Nominal cell voltages for lithium-ion, lead acid and nickel-based batteries are 3.6 V, 2 V and 1.25 V respectively [6]. For example, nominal (or reference) voltage of a lithium-ion battery is calculated by taking a fully charged battery of about 4.20 V, fully discharging it to about 3.00 V at a rate of 0.50 C while measuring the average voltage [9].

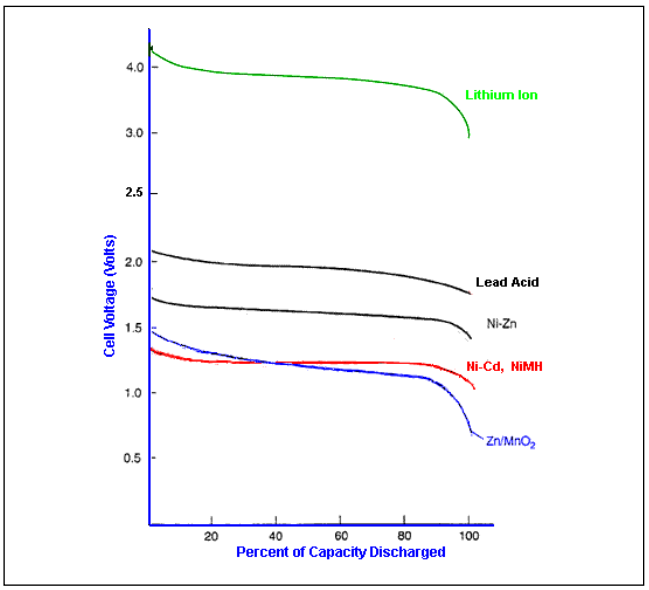

Fig. 1.4. Typical discharge curves of batteries composed by different chemistries [10]

1.2.4. Internal resistance

The ohmic resistance represents the opposition to current flow produced by the electrodes and the electrolyte (Fig. 1.5). It is not a simple ohmic resistor. It depends on the way the battery is used and on SoC and SoH. Internal resistance determines the battery's power output. Internal resistance must to be small to obtain a high power output.

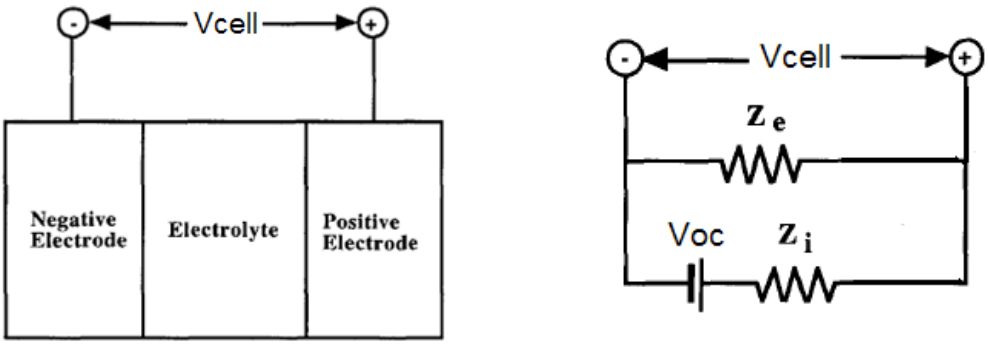

Fig. 1.5. On the left: simple model of an electrochemical cell. On the right: simple equivalent model of a battery indicating the effect of the internal impedance (*Zi*) upon the output voltage and including electronic leakage through the electrolyte (*Ze*). V_{OC}-V_{cell} is the overpotential voltage of the battery ($\Delta\phi$) [11]

The total impedance of the battery is a complex parameter and it is difficult to interpret since the AC behaviour of a battery can only be approximated by an equivalent circuit of many components (Fig. 1.6).

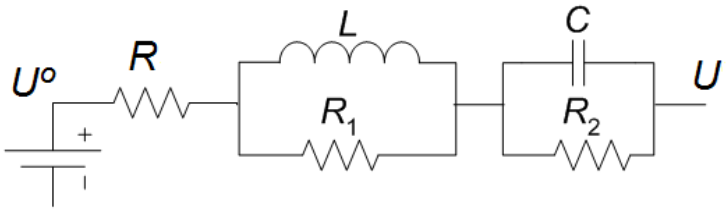

Fig. 1.6. Electrical model of the battery [5]
(U_o represents V_{OC} and U represents V_{cell})

1.2.5. Self-Discharge

When a battery is idle at open circuit, the positive and/or the negative electrode suffers a gradual loss of charge. This effect is called self-discharge. There is a huge difference on self-discharge rates for different types of secondary batteries. It depends on system and construction but typical values range from 2 % to 30 % per month at ambient temperature. Lithium-ion batteries offer about 5 % to 10 % per month.

1.3. Typical chemistries of secondary batteries and charging methods

An overview of lead acid batteries, nickel-based batteries and lithium batteries will be presented in this section. Also some typical charging methods will be described.

1.3.1. Lead-acid batteries

Lead-acid battery is the oldest secondary system, widely used, and well known. It is characterized by the fact that lead is used in both electrodes as the active material and sulphuric acid is used as electrolyte [4].

The lead-acid battery has one of the lowest energy densities, making it unsuitable for portable devices. In addition, the performance at low temperatures is marginal. The high lead content makes the lead-acid environmentally unfriendly.

Despite having a very low energy-to-weight ratio and a low energy-to-volume ratio, they can supply high surge currents, thus having a relatively large power-to-weight ratio. These features, along with their low cost, make them attractive to be used to provide the high current required by automobile starter motors.

1.3.1.1 *Sealed lead-acid (SLA)*

To improve lead-acid batteries, a maintenance-free lead-acid battery that could operate in any position was developed. The liquid electrolyte is gelled into moistened separators and the enclosure is sealed. Safety valves allow venting during charge, discharge and atmospheric pressure changes [9].

1.3.2. Nickel-based batteries

Nickel/cadmium, and nickel/metal hydride batteries are the most important members of this group. A common feature of these battery systems is the use of nickel-hydroxide electrode in the positive one [4].

NiCd batteries have been in technical use nearly as long as lead-acid batteries. They are based on an alkaline aqueous electrolyte (usually it is diluted potassium hydroxide). Their development started in the beginning of the twentieth century. They still have a strong market position, mainly in its sealed version as a portable power source, but also as a flooded battery in traction and stationary applications.

Initially, NiMH development was motivated by the substitution of cadmium because of its toxicity. The higher storage capability, however, turned the NiMH battery to more than only a substitute and opened the path to many other

applications for the new battery. NiMH batteries, unlike NiCd, do not suffer from memory effect.

Some disadvantages of NiMH batteries compared to NiCd should be considered:

- Higher price
- At low temperatures and at high loads the desorption rate of the hydrogen can be a limitation
- NiMH batteries heat up more than NiCd batteries, when used in heavy cycling schedules

1.3.3. Lithium batteries

The first lithium-based batteries were primary batteries (they became commercially available in the early 1970s). They were based on pure metallic lithium negative electrodes. Then, it was attempted in the 1980s to develop also rechargeable lithium cells (secondary batteries). Because of the inherent instability of lithium metal, especially during charge, research shifted to a non-metallic lithium battery using lithium ions. Although slightly lower in energy density than lithium metal, lithium-ion is safe if certain precautions are met when charging and discharging. In 1991, the Sony Corporation commercialized the first Li-ion battery.

1.3.3.1 *Lithium-ion batteries*

The energy density of lithium-ion is typically twice that of the standard nickel-cadmium. The load characteristics are reasonably good and behave similarly to nickel-cadmium in terms of discharge. The high cell voltage of 3.6 volts allows battery pack designs with only one cell. A nickel-based pack would require three 1.2 volt cells connected in series.

Lithium-ion is a low maintenance battery, an advantage that most other chemistries cannot claim. There is no memory effect and no scheduled cycling is required to prolong the battery's life. Memory effect, in short, refers to the battery's loss of capacity due to partial discharge cycles. No scheduled cycling means that the battery doesn’t need to be fully discharged before being charged. Moreover, as the battery prefers a partial rather than a full discharge, frequent full discharges should be avoided when possible. In addition, the self-discharge is less than half compared to nickel-cadmium. Moreover, lithium-ion cells cause little harm when disposed.

Despite its overall advantages, lithium-ion has its drawbacks. They require a protection circuit to maintain safe operation. Built into each pack, the protection circuit limits the peak voltage of each cell during charge and prevents the cell voltage from dropping too low during discharge. In addition, the cell temperature is monitored to prevent excessive temperature variations. They usually incorporate an internal thermistor for security purposes. These thermistors

prevent from overheating when charging or discharging the battery in a normal use and in some cases they are used to compensate voltage measurements from temperature variations [6].

Positive and negative electrodes

Nowadays, most lithium-ion batteries have shifted to graphite as negative electrode; Sony's original version used coke instead. Graphite-based electrode provides a flatter discharge voltage curve than coke.

The most widely used chemistries for the positive electrode are cobalt and manganese (also known as spinel). Whereas cobalt has been in use longer, manganese is inherently safer. In addition, the raw material for manganese is lower than cobalt. However, manganese offers slightly lower energy density, suffers capacity loss at temperature above 40ºC and ages quicker than cobalt (Table 1.1). Chemicals and additives help to balance the critical trade-off between high energy density, long storage time, extended cycle life and safety.

Table 1.1. Comparison of manganese and cobalt as positive electrodes [6]

	Cobalt	Manganese (Spinel)
Example of energy density (Wh/Kg)	140	120
Safety	On overcharge, the cobalt electrode provides extra lithium, which can form into metallic lithium, causing a potential safety risk if not protected by a safety circuit	On overcharge, the manganese electrode runs out of lithium causing the cell only to get warm. Safety circuits can be eliminated for small 1 and 2 cell packs
Temperature	Wide temperature range. Best suited for operation at elevated temperature	Capacity loss above 40ºC. Not as durable at higher temperatures
Life Expectancy	300 cycles. 50 % capacity at 500 cycles	May be shorter than cobalt
Cost	Raw material relatively high; protection circuit adds to costs	Raw material 30 % lower than cobalt. Cost advantage on simplified protection circuit

1.3.3.2 *Lithium-polymer batteries*

Lithium–polymer batteries (LPB) use intercalated carbon for the negative electrode, a polymer for the electrolyte, and metallic lithium that is deposited as a thin film as the positive electrode. The original design uses a dry solid polymer

electrolyte. This electrolyte does not conduct electricity but allows the exchange of ions. The polymer electrolyte replaces the traditional porous separator, which is immersed on the electrolyte. The dry polymer design offers simplifications with respect to fabrication, ruggedness, safety and thin-profile profile. There is no danger of flammability because no liquid or gelled electrolyte is used.

Unfortunately, the dry Li-polymer suffers from poor conductivity. The internal resistance is too high and cannot deliver the current bursts needed for modern communication devices. Although heating the cell to 60°C and higher increases the conductivity to acceptable levels. This requirement, however, is unsuitable for portable applications. Most of the commercial Li-polymer batteries are a hybrid: some gelled electrolyte has been added to the dry polymer. The correct term for this system is *Lithium Ion Polymer* (Li-ion polymer or LiPo).

Although the characteristics and performance of the two systems (Li-ion and Li-ion polymer) are very similar, the Li-ion polymer is unique in that the solid electrolyte replaces the porous separator. The gelled electrolyte is simply added to enhance ion conductivity. Li-ion polymer batteries allow then very thin geometries [6].

1.3.3.3 *Lithium-cell reactions*

The lithium-ion technique consists on lithium ions exchange between positive and negative electrodes during discharge and charge. The negative electrode of carbon in the graphitic form contains the lithium in the charged state and delivers it to the positive electrode made from cobalt oxide CoO_2 during discharge (Fig. 1.7). The lithium ions migrate during cycling forth and back between the two host lattices of C_x and CoO_2. The following reaction scheme shows this in a simplified manner:

$$\text{Negative electrode: } LiC_6 \rightarrow C_6 + Li^+ + e^- \qquad (1.6)$$

$$\text{Positive electrode: } CoO_2 + Li^+ + e^- \rightarrow LiCoO_2 \qquad (1.7)$$

$$\text{Cell: } LiC_6 + CoO_2 \rightarrow C_6 + LiCoO_2 \qquad (1.8)$$

For charge and discharge the arrows have to be reversed. This back and forth of the lithium ions is named ‘rocking chair’ or ‘swing’ principle [4].

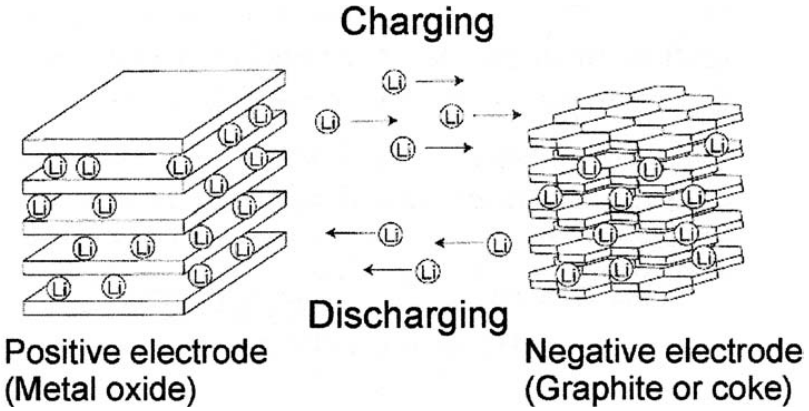

Fig. 1.7. Charging/discharging lithium-ion batteries [4]

Apart from the desired main chemical reactions, every electrochemical system is strained by secondary reactions (oxidation and corrosion), which cause a self-discharge [4]. If the secondary reaction occurs while discharging the battery, some of the charge (current that would normally flow to the load) is used by the secondary reaction. Similarly, during charge secondary reactions use charge intended to drive the main battery reactions. These phenomena will be related to SoH.

1.3.4. Charging methods

Some charging methods have certain advantages depending on battery type. Given the battery chemistry, a particular charging profile may be need. Selecting the right charging method extended performance, battery cycles and the life of your battery will be ensured [12].

1.3.4.1 *Constant-current chargers*

This kind of chargers varies the voltage they apply to maintain a constant current flow and they switch off themselves when the voltage reaches the level of a full charge. It is usually used for NiCd and NiMH batteries.

1.3.4.2 *Constant-voltage chargers*

Constant-voltage chargers are basically dc power supplies that provide the dc voltage to charge the battery. They are used for lead-acid cells in car starter batteries and backup power systems. In addition, Li-ion cells often use constant-voltage systems, although these are usually more complex with added circuitry to protect both the batteries and the user. This is constant-voltage charger but current limited (constant current/constant voltage method).

Charging lithium-ion batteries

Constant current/constant voltage algorithm is used as optimum charge method of lithium-ion batteries.

The first stage consists on a constant current step. Then, the battery keeps charging until the maximum charge voltage is reached. At that time, current starts to decrease while maintaining the voltage constant until the end-of-charge current[1] is reached (Fig. 1.8).

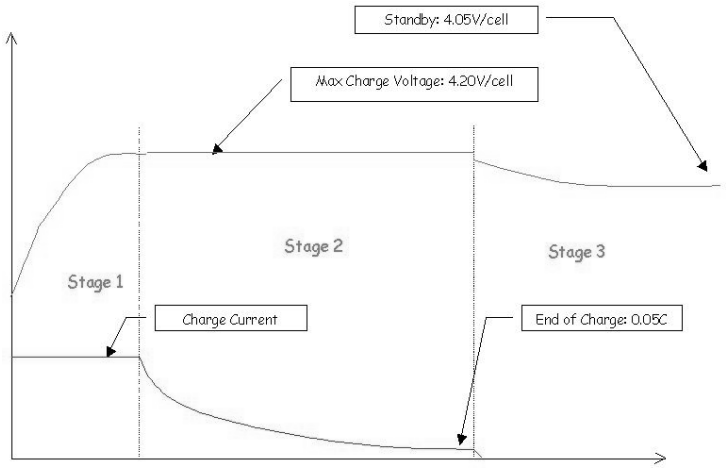

Fig. 1.8. Constant current/constant voltage algorithm used in Li-ion batteries [13]

1.3.4.3 *Taper-current chargers*

They supply an unregulated constant-voltage source. This is not a controlled charge. The current diminishes as the voltage increases and there is a serious danger of damaging the cells through overcharging. To avoid that problem, charging rate and duration should be limited. This charging method is only suitable for large industrial lead-acid batteries.

1.3.4.4 *Pulsed chargers*

Current is delivered to the battery in pulses. This method can reduce unwanted chemical reactions at the electrode surface.

[1] All this data is specified by the manufacturer of the battery

1.4. Heat effects

While charging or discharging a battery, heat (Q_{Total}) is generated due to different reasons. The current flow generates heat through the Joule effect (Q_P) due to ohmic resistances present in the electrodes and the electrolyte. Furthermore, the electrochemical reaction also adds an additional term (Q_S). Finally, heat transfer to the ambient is also considered in the heat balance (Q_B) (1.9).

$$\frac{dQ_{Total}}{dt} = C_{Li} \cdot \frac{dT_{cell}}{dt} = \frac{dQ_P}{dt} + \frac{dQ_S}{dt} - \frac{dQ_B}{dt} \tag{1.9}$$

Where, C_{Li} is the heat capacity of the cell (J/K) and T_{cell} is the cell temperature (K).

The energy dissipated inside the battery represented by Q_P is due to the voltage drop across the internal resistor of the battery (Joule effect) (1.10).

$$\frac{dQ_P}{dt} = I \cdot (V_{OC} - V_{cell}) = I^2 \cdot R_\eta \tag{1.10}$$

Where, V_{OC} is the open-circuit voltage (V), V_{cell} is the cell voltage under current flow (V), I is the current flowing through the battery (A) (by convention it is considered to be positive during discharge and negative during charge) and R_η is the overpotential resistance (Ω) (refer to section 1.2.4). The difference V_{OC}-V_{cell} is the overpotential voltage $\Delta\phi$.

Q_S is described by the entropy change (ΔS in $J \cdot mol^{-1} \cdot K^{-1}$) (1.11).The product $T \cdot \Delta S$ is called the reversible heat effect. It represents the heat absorption or heat emission related to the cell reaction. Therefore, in lithium batteries the sign of Q_S is different between charge and discharge processes.

$$\begin{gathered} \Delta S = n \cdot F \cdot \frac{dV_{OC}}{dT} \\ \frac{dQ_S}{dt} = -T_{cell} \cdot \Delta S \cdot \frac{I}{F} = -T_{cell} \cdot \frac{dV_{OC}}{dT} \cdot I \end{gathered} \tag{1.11}$$

Where, n is the number of exchanged electrons (that is equal to 1 for lithium batteries as inferred from (1.6) and (1.7)) and F is the Faraday constant (96485 A·s/equivalent).

ΔS is a thermodynamic parameter of an electrochemical reaction together with the enthalpy of reaction (*ΔH*) and the free enthalpy of reaction (*ΔG*) (1.12). Thermodynamic parameters do not depend on the reaction path, but depend only on the different energy levels between the final and initial components.

$$\Delta \mathrm{H} - \Delta \mathrm{G} = \mathrm{T} \cdot \Delta S \tag{1.12}$$

Where, *ΔH* represents the amount of energy released or absorbed. It describes the maximum heat generation, provided that the chemical energy is converted into heat by 100 %. *ΔG*, also called change of Gibb's free energy, describes the maximum amount of chemical energy that can be converted into electrical energy and viceversa. *ΔG* and *ΔH* depend on the concentrations of the reacting components.

Finally, as said above, Q_B is the heat transferred to the ambient (1.13).

$$\frac{dQ_B}{dt} = A \cdot h \cdot (T_{cell} - T_{room}) \tag{1.13}$$

Where, *A* is the surface area of the battery, *h* is the battery heat transfer coefficient and T_{room} is the ambient temperature. This term will be strongly dependent on geometrical distribution and environmental conditions.

Concluding, in some cases the total heat energy generated will be larger or smaller than the Joule effect depending on the sign of the heat generated by the entropy change.

1.4.1. Thermal impedance

Thermal impedance is a novel parameter introduced in 2008 [2]. It was used to describe thermal behaviour of NiMH batteries.

Thermal impedance is defined as a function that takes into account battery temperature variations. It can be derived similarly to electric impedance functions. The square of current is treated as a current equivalent and heat-flow as a voltage equivalent (1.14).

$$Z_t(w) = \frac{\mathcal{F}\left\{\frac{dQ_{Total}}{dt}\right\}}{\mathcal{F}\{i^2(t)\}} \tag{1.14}$$

$\mathcal{F}\{\ldots\}$ means the Fourier Transform.

If the battery is charged or discharged by a constant current, the denominator can be expresses as follows:

$$i^2(t) = i^2(t) \cdot \theta(t) \tag{1.15}$$

Where, $\theta(t)$ is the Heaviside step function.

Regarding to the denominator and considering different heat terms an equation that describes the total heat flow for NiMH batteries is obtained (1.16) [2].

$$\begin{aligned} \frac{dQ_{Total}(t)}{dt} &= I \cdot V_{cell} \cdot \xi + I \cdot \left(\frac{V_{cell} - E_0 - T_{cell} \cdot \Delta S}{n \cdot F}\right) \cdot (1 - \xi) \\ &\approx I \cdot \left(\frac{V_{cell} - E_0 - T_{cell} \cdot \Delta S}{n \cdot F}\right) + I \cdot \xi \cdot \left(\frac{E_0 + T_{cell} \cdot \Delta S}{n \cdot F}\right) \\ &= I \cdot \left(\frac{I \cdot R - \Delta\phi - T_{cell} \cdot \Delta S}{n \cdot F}\right) + I \cdot \xi \cdot \left(\frac{E_0 + T_{cell} \cdot \Delta S}{n \cdot F}\right) \end{aligned} \tag{1.16}$$

Where, ξ is the current ratio of the secondary reaction, E_0 is the standard voltage of the battery, $\Delta\phi$ is the overpotential and R is the sum of ohmic resistance.

It is assumed that, between 40 % and 60 % SoC, ξ and $\Delta\phi$ increase approximately linear (1.17).

$$\begin{aligned} \xi &= \xi_0 + k_\xi \cdot t \\ \Delta\phi &= \Delta\phi_0 + k_{\Delta\phi} \cdot t \end{aligned} \tag{1.17}$$

Where, $\Delta\phi_0$ is the initial value of $\Delta\phi$, $k_{\Delta\phi}$ is the slope of the overpotential, ξ_0 is the initial value of ξ, k_ξ is the slope of the ratio of current for the secondary reaction and t is the sampling time.

By combining equations (1.17) and (1.16), the latter could be decomposed in two terms: one that is time dependent and one that no depends on time (1.18).

$$\begin{aligned} \frac{dQ_{Total}(t)}{dt} &= I^2 \cdot \left(R + \frac{\Delta\phi_0}{I} - \frac{T_{cell} \cdot \Delta S}{n \cdot F \cdot I} + \xi_0 \cdot \frac{E_0 + T_{cell} \cdot \Delta S / n \cdot F}{I}\right) \\ &\quad + I^2 \cdot t \cdot \left(k_\xi \left(\frac{E_0 + T_{cell} \cdot \Delta S / n \cdot F}{I}\right) + \frac{k_{\Delta\phi}}{I}\right) \end{aligned} \tag{1.18}$$

Equation (1.18) can be represented by a thermal model composed by a resistance and a capacitor (Equation (1.19) and Fig. 1.9).

$$\frac{dQ_{Total}(t)}{dt} = I^2 \cdot R_t + \frac{I^2 \cdot t}{C_t} \tag{1.19}$$

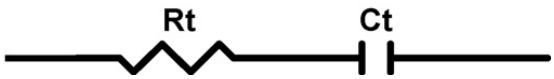

Fig. 1.9. Equivalent thermal model of the battery [2]

CHAPTER 2. DEVICES AND METHODS

In this chapter, the main features of the battery used in that project will be listed. Furthermore, the equipment and the methods employed will be described. Current, voltage, temperature and impedance measurements were carried out. Also the procedure of charge and discharge the battery is explained in this section.

2.1. Battery

The tests were carried out in a LIP 533048 AJ battery, which is a lithium-ion cell manufactured by Varta Microbattery. It is based on cobalt technology with a nominal voltage of 3.7 V and 740 mAh. It includes a 10 kΩ NTC thermistor inside for security purposes.

The main data of the battery involved in that work is shown on Table 2.1 (refer to ANNEX).

Table 2.1. Main data of LIP 533048 AJ from Varta Microbattery [14]

Type Designation	LIP 533048 AJ
Negative electrode	Carbon in the graphitic form
Positive electrode	Lithium cobalt oxide
Nominal Voltage (V)	3.7
Typical Capacity (mAh)	740
Dimensions [w] [t] [L] (mm)	[30.0 +0/-0.6] [5.3 Max.] [47.8 +0/-0.6]
Weight, approx. (g)	17
Charge Voltage (V)	4.20 (+/- 50 mV)
Charging Cut-Off by min. current (mA)	0.02C
Discharge Cut-Off Voltage (V)	3.0
Operating Temperature (ºC)	Charge: 0 to 45 – Discharge: -20 to 45
Internal Thermistor	10 kΩ NTC

2.2. Charge and discharge processes

In this chapter, it will be explained how battery cycles were scheduled. Procedures used to carry out the measurements. and all equipment involved in this study will be described.

2.2.1. The Cadex C7200-C

A battery analyzer was used for charge and discharge processes. This type of device offers the possibility to choose between different charging methods depending on battery chemistry. Also some parameters can be configured as voltage or current limits, charge rates or battery's capacity. Particularly, C7200-C battery analyzer from Cadex Electronics [13] was used.

It has many different programmes for different purposes (charge/discharge the battery, SoC and SoH estimation or resistance measurement). A user can also make custom programs with different steps (Fig. 2.1).

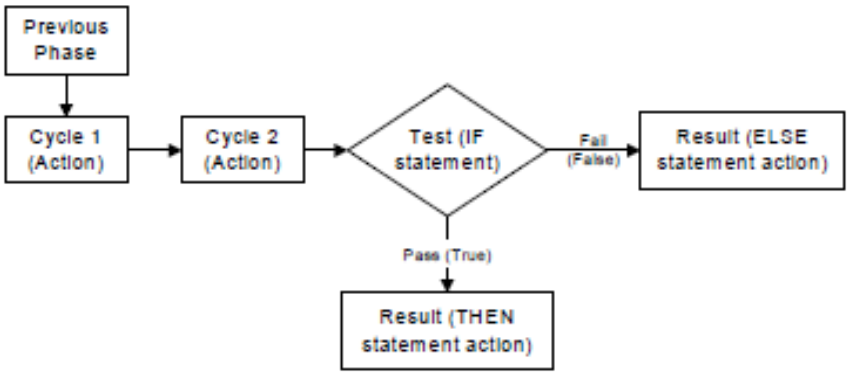

Fig. 2.1. Custom program processes, phases 1 through 5 [13]

HyperTerminal or BatteryShop^{TM} software from Cadex could be used to transfer data from battery analyzer to the computer through a U232 serial connection. In both cases, data is obtained every 60 seconds with no possibility to change it. Among other things as SoH or internal resistance (in the case of BatteryShop^{TM}), voltage readings and current readings can be obtained from it.

C7200-C uses a constant current/constant voltage algorithm (refer to section 1.3.4.2) to optimum charge and discharge lithium-ion batteries as specified on the datasheet of the battery. Some battery parameters have to be configured in the battery analyzer before starting using it. This information is stored on the C-code of the specific battery and it contains the chemistry, voltage and rating (Table 2.2).

Table 2.2. C-code configured in C7200-C to charge a Li-ion battery (LIP 533048 AJ Microbattery from VARTA)

Parameter	Default C-code	Used C-code
Target capacity	80 %	80 %
Chemistry	Li-ion	
Voltage (V)	3.60	3.60
Capacity (mAh)	750	750
Charge C-rate	1.00 C	1.00 C and 0.50 C
Discharge C-rate	1.00 C	1.00 C and 0.50 C
Temperature sensing (ºC)	0 – 45	0 – 45
Max. standby voltage (V/cell)	4.05	4.05
Max. charge voltage (V/cell)	4.20	4.20
End-of-charge	0.05 C	0.02 C
End-of-discharge (V/cell)	3.00	3.00

A traditional test method used to obtain the battery resistance is the 1000 Hertz Method. It injects a 1000Hz signal to calculate the resistance. In this method, resistance readings may be subject to battery reactance. C-series battery analyzers from Cadex use a DC OhmTest method. The battery is discharged for 10 seconds at a low current, followed by a 3 seconds discharge at a higher current (Fig. 2.2). The resistance is calculated using Ohm's law. However, these two methods are only able to provide an estimation of the internal resistance [13].

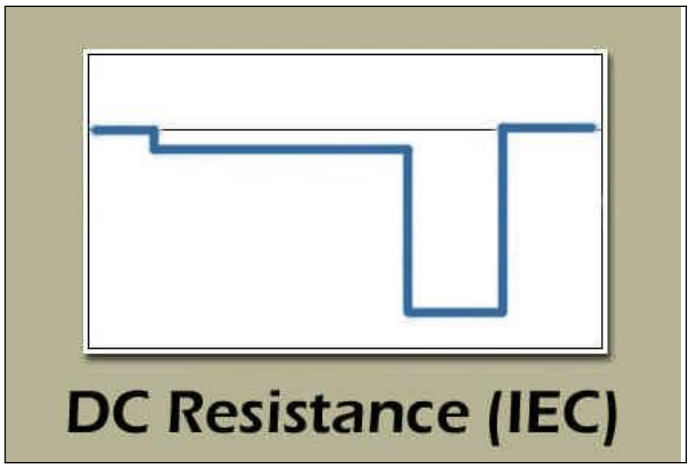

Fig. 2.2. Discharge current profile of DC OhmTest used to calculate internal resistance by C7200-C battery analyzer [13]

2.2.2. Procedure of charge/discharge

A cycle counts of a charge process followed by a discharge. Cycles were configured in the battery analyzer and measurements were conducted by two different charge rates: 1.00C and 0.50C. In both cases, a resting period of 15 minutes was programmed between every charge and discharge and viceversa to allow the battery to recover towards V_{OC}.

During charge and discharge processes, the battery was kept thermally isolated from the environment with expanded polystyrene. In that conditions, there is no heat transferred to the ambient (adiabatic conditions and thus, Q_B=0) (refer to section 1.4).

2.2.3. Voltage measurements during charge and discharge

Agilent 34970A data acquisition system [15] is used to collect voltage readings. It is configured with a high input resistance (higher than 10 MΩ) to isolate as much as possible the battery from the measurement equipment. The resolution is selected to be six and a half bits and PLC (Power Line Cycles) equal to 10.

Data is transferred to the computer by GPiB-USB connector. Agilent BenchLink Data Logger is the software provided by the manufacturer and it is used to configure the device and to obtain readings of the measurements.

2.2.4. Current measurements

Current readings are obtained by C7200-C battery analyzer during charge and discharge processes. It gives a reading every 60 seconds and they are recorded on the computer.

Current was calibrated with TCPA300 current probe amplifier [16]. The amplifier converts the sensed current into a proportional voltage signal that you can measure directly with an oscilloscope (Fig. 2.3). Specifically, DSO3062A Digital storage oscilloscope from Agilent Technologies was used [15].

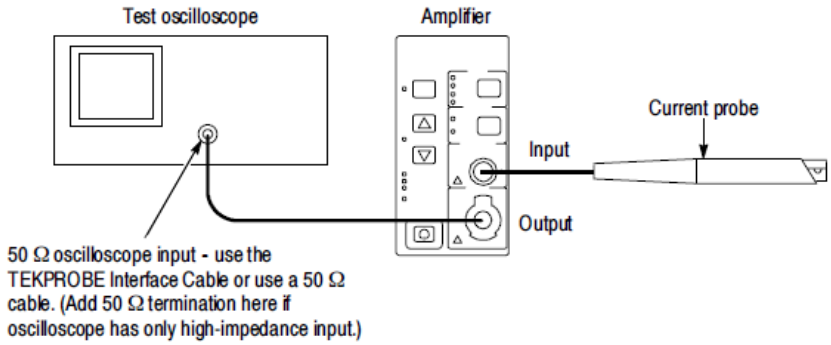

Fig. 2.3. Typical TCPA300 configuration system [16]

2.3. Temperature measurements

Temperature variations inside the battery were measured with the battery thermistor. Two different situations were distinguished; on the one hand, temperature changes produced by a current flowing through the battery during charge and discharge processes and on the other hand, temperature changes induced on the battery by temperature environmental change.

2.3.1. Temperature changes during charge and discharge processes

Temperature was monitored while charging and discharging the battery by different currents. It was obtained by a pre-defined function in Agilent 34970A Data acquisition/Switch unit that calculates the temperature from voltage measurements applying the characteristic equation of a 10 kΩ NTC thermistor (Table 2.1).

2.3.2. Induced temperature cycles

Environmental temperature was controlled with a thermal water bath. A micro magnetic mixer was used to heat and mix the water in order to monitor V_{OC} changes with temperature. Tests with different SoCs were carried out as V_{OC} varies with SoC and temperature.

The micro magnetic mixer, MicroMagMix provided by Ovan [17], has a temperature range that goes from 0 ºC to 400 ºC. It is formed by a heating plate, a test tube full of water, a temperature probe, a panel from which the temperature can be changed and an agitator that unify water temperature (Fig. 2.4). To immerse the battery on the water, it was isolated inside a plastic bag.

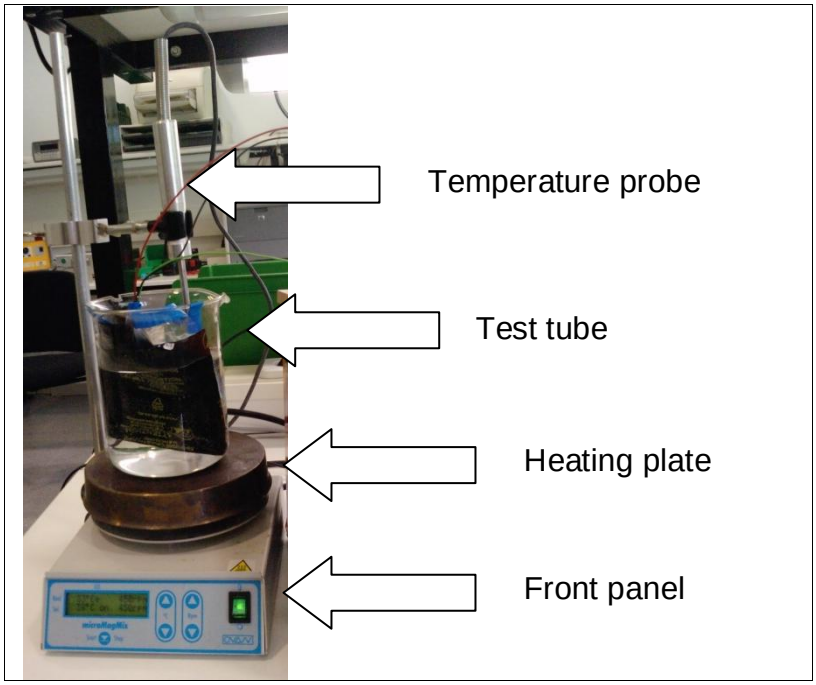

Fig. 2.4. Micro magnetic mixer

2.3.2.1 *V_{OC} and dV_{OC}/dT*

Temperature changes are induced on the battery by thermal bath and V_{OC} is measured. This procedure is performed as a function of SoC at six different points. Since V_{OC} takes a long time to be stabilized it was allowed to rest 24 hours.

2.4. Impedance measurement

An impedance spectrometer (4294A from Agilent) was used to measure battery impedance. A special circuit is required to do that measurement (Fig. 2.5). Two capacitors (C_1 and C_2) block DC current flowing into the instrument. The value of C_1 should be calculated using the minimum measurement frequency.

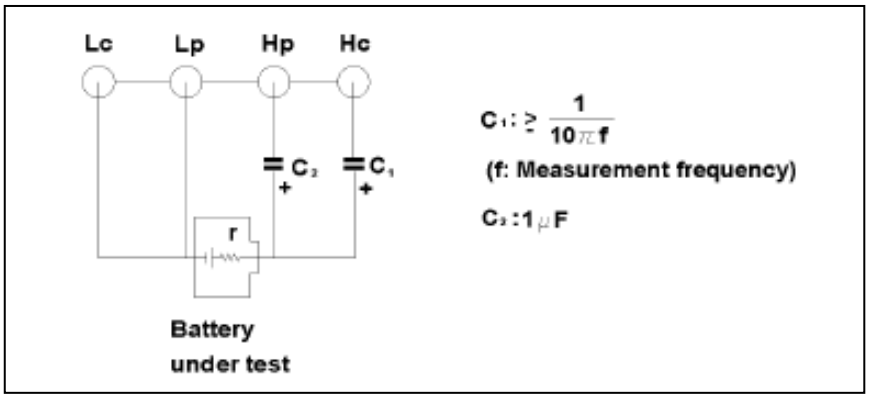

Fig. 2.5. Battery measurement setup [18]

CHAPTER 3. RESULTS AND DISCUSSIONS

3.1. SoC and SoH definitions

SoC was defined in equations (1.4) and (1.5). However, this definition does not consider the interrelation with SoH. Thus, we propose a new definition for SoC as the ratio between the available capacity and the present capacity of the battery (3.1). For every charge or discharge cycle the range of values always goes from 0 % to 100 % (independently from the aging of the battery).

$$\mathrm{SoC} = \frac{\text{Available capacity}}{\text{Present capacity}} \tag{3.1}$$

We define SoH as the ratio between present capacity of the battery and the original one (3.2).

$$\mathrm{SoH} = \frac{\text{Present capacity}}{\text{Original capacity}} \tag{3.2}$$

3.1.1. Time to SoC conversion

For every cycle, injected or extracted charge is calculated according to (3.3). A first consideration is that the battery was empty before charging (SoC=0 %) because of a previous full discharge to a minimum voltage of 3V. Then, after charging process, the total injected charge is considered to be SoC equal to 100 %. Once those values are obtained, all points between 0 % and 100 % SoC are scaled by SoC equation (3.1).

$$\mathrm{C_{Ah}} = \int_0^t \mathrm{I(t)} \cdot \mathrm{dt} \tag{3.3}$$

A similar behaviour occurs with discharge process. The initial condition is that the battery is fully charged and the minimum charge at the end of discharge is considered to be SoC equal to 0 %. Other intermediate values are scaled.

Time to SoC conversion is useful to compare processes that have different time duration.

3.2. Voltage, current and temperature

Battery was charged and discharged at constant current at 0.50C and 1.00C at room temperature of 25ºC. It has to be pointed out that C7200-C battery analyzer gives non-symmetrically current amplitudes between charge and discharge processes (Table 3.1). Cell voltage was monitored in both cases (0.50C and 1.00C) while discharging the battery. Temperature variations are different when charging than when discharging the battery. During charge, temperature first decreases and later increases while during discharge, it increases during the whole process (Fig. 3.1 and Fig. 3.2).

Table 3.1. Current amplitudes during charge and discharge vs. charge rate

Charge rate	*I* during charge (mA)	*I* during discharge (mA)
1.00C	840	720
0.50C	332	400

When charging the battery (Fig. 3.1), current remains constant up to 70 % of the SoC. Then, it starts to decrease as expected when using constant current/constant voltage algorithm because it keeps constant voltage after this stage. Regarding to cell voltage values a variation between 3.79 V and 4.21 V is observed. It matches well with the requirements of the battery (refer to section 2.1).

On the first 25 % SoC, as illustrated in Fig. 3.1, temperature decreases in approximately half a degree. Between 25 % and 70 % SoC, temperature rises approximately 1.5 K. At that point, temperature starts to decrease because current is smaller every time until the end of charge. There is a correspondence between the point at which temperature starts to rise (approximately 25 % SoC) with a slope increase in the voltage curve.

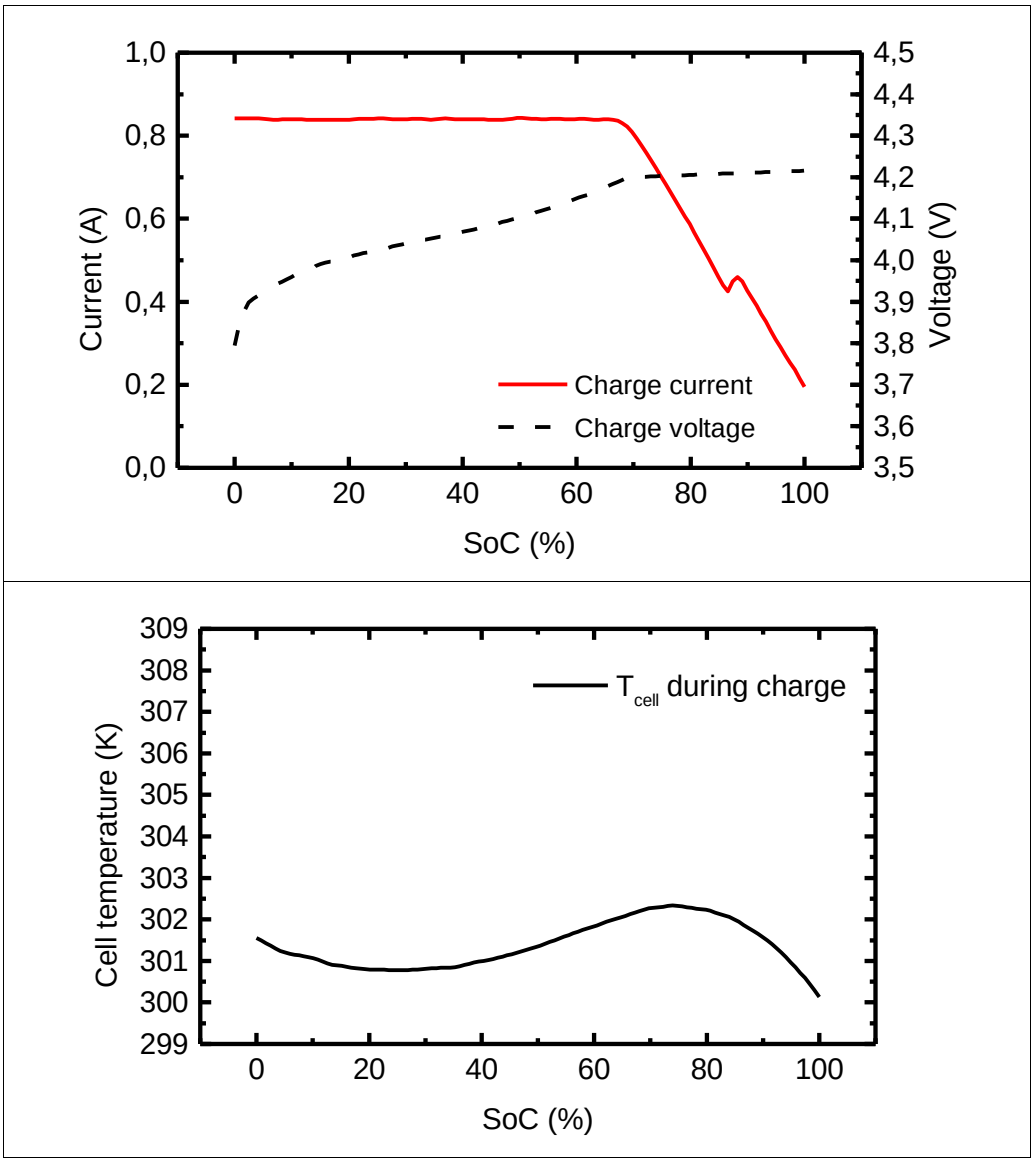

Fig. 3.1. Voltage, current and cell temperature for battery charged at 1.00C rate. Notice that temperature decreases at first to increase only in the range of 30 to 80 % of the SoC. Room temperature: 298K (25ºC)

During discharge process, current remains constant for all SoC (see Fig. 3.2). Discharge voltage ranges from 3.93 V to 3.11 V. Voltage cannot decrease below 3 V so these are correct values. In that case, temperature rises almost 8 K that is higher than when charging the battery.

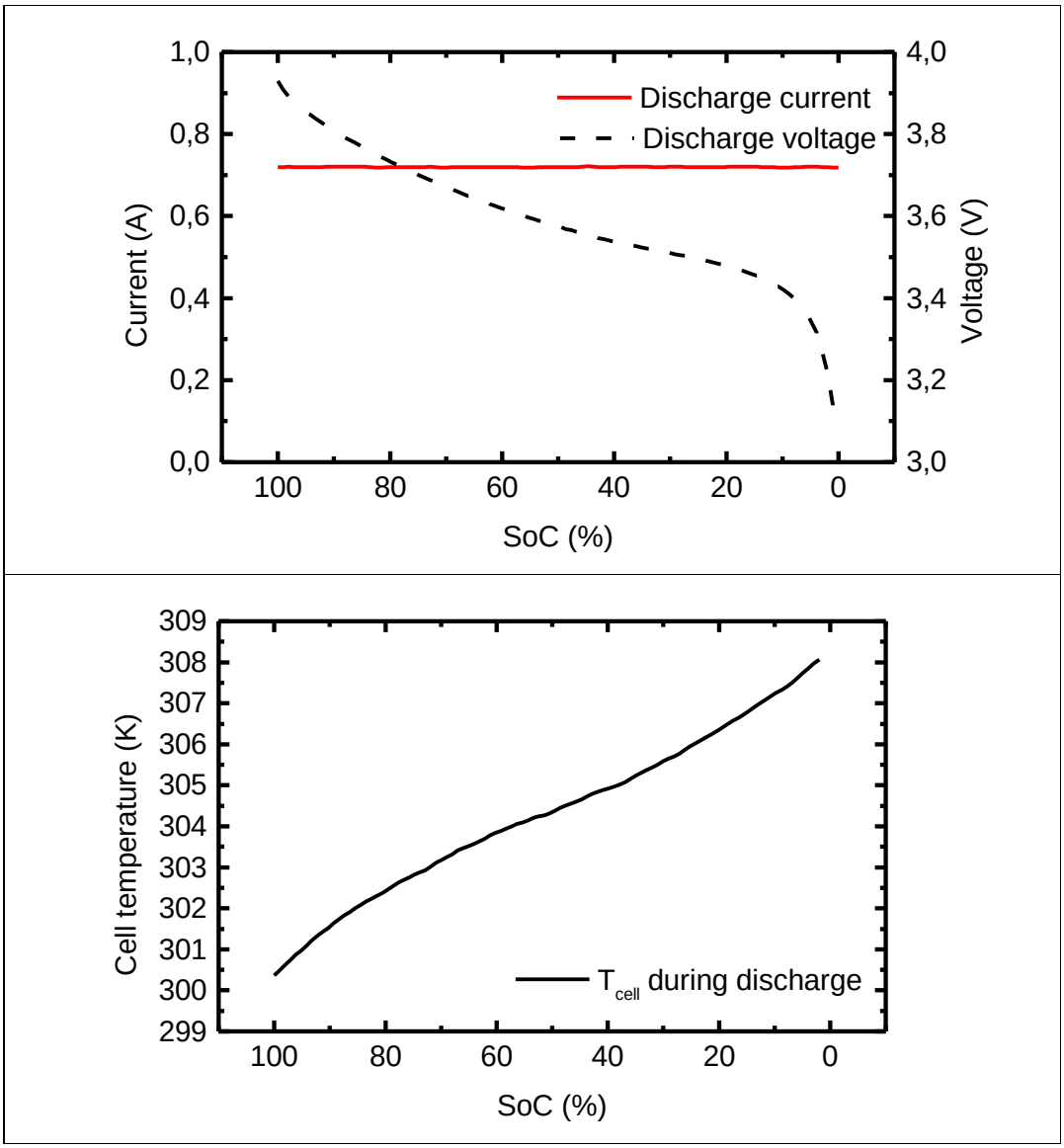

Fig. 3.2. Voltage, current and cell temperature for battery discharged at 1.00C. In this case, temperature increases in the whole range. Room temperature of 298.15K (25ªC)

3.3. Heat produced by Joule Effect

The heat produced by the overpotential voltage has been calculated using two different methods: the *V-I* characteristics at constant-current discharge and the difference between the open-circuit voltage and the cell voltage.

3.3.1. From *V-I* characteristics

When using *V-I* slope method, the overpotential resistance needs to be calculated as a first step to calculate dQ_P/dt (1.10). This method consists in measuring V_{cell} and discharge current at different discharge rates (we considered 0.50C and 1.00C) to obtain the *V-I* curve (Fig. 3.3). The slope of the

V-I curve for every individual SoC gives the overpotential resistance (Fig. 3.4) [1]. Another way to understand how resistance is calculated with this method is the following: the battery is loaded with a current I_1 (0.50C in our case) and voltage $(V_{cell})_1$ is monitored. This process is repeated for a higher current I_2 (1.00C in this project) and the battery voltage is found to be reduced to the value $(V_{cell})_2$,. The internal resistance R_η is then calculated according to (3.4) [4].

$$R_\eta = \frac{(V_{cell})_1 - (V_{cell})_2}{I_2 - I_1} \tag{3.4}$$

Cell resistance values during charge upper 70 % SoC are not represented because charge current is no more a constant value (Fig. 3.1) and hence they cannot be calculated by this method.

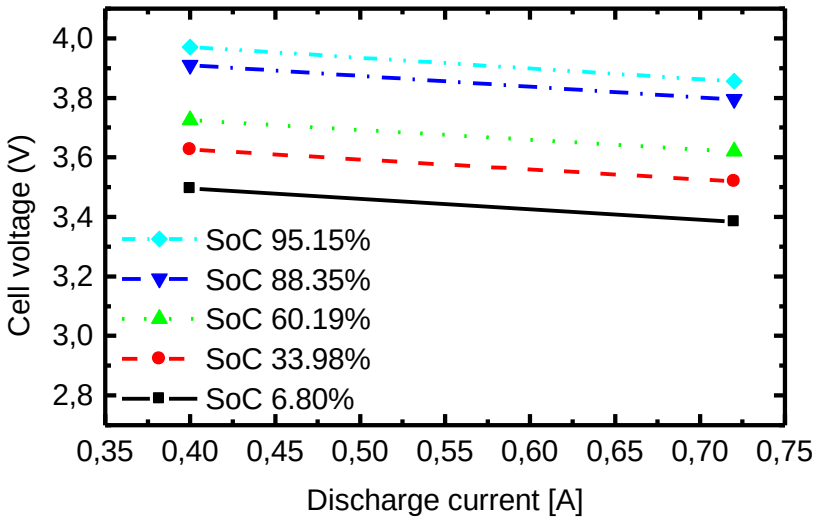

Fig. 3.3. Determination of R_η using constant discharge currents of 400mA and 720mA. The slope of the *V-I* characteristics for every SoC determines the resistance

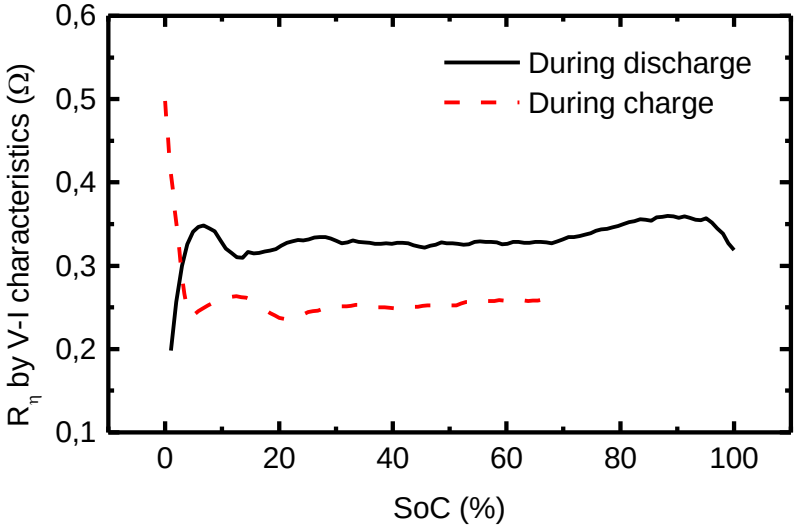

Fig. 3.4. Cell resistance by *V-I* characteristics as a function of SoC

Both for charge and discharge processes resistance remains almost constant from empty to full charge. R_η is approximately 330mΩ during discharge and 250mΩ during charge. The denominator in equation (3.4), defined by the difference of currents at different charge or discharge rates, is higher during charge (Table 3.1). This causes the resistance to increase during charge with respect to discharge process. Thus, the achieved values for cell resistance are coherent with what can be expected for lithium-ion batteries (refer to section 3.8).

3.3.2. From open-circuit voltage

In this method, the difference between V_{OC} and V_{cell} (overpotential voltage $\Delta\Phi$) is calculated graphically. Once it is done, the overpotential resistance is obtained by dividing it by the discharge current according to (1.10).

The difference between discharge voltage and open-circuit voltage during discharge is almost constant for all SoC range (Fig. 3.5). Same situation occurs with charge voltage until 70% SoC (Fig. 3.6). Then, V_{OC} and V_{cell} do not have anymore the same shape. It is mainly because of the method employed when charging the battery; voltage is forced to be constant in this range. For further calculations voltage drop is considered to be constant either for charge as for discharge (Table 3.2).

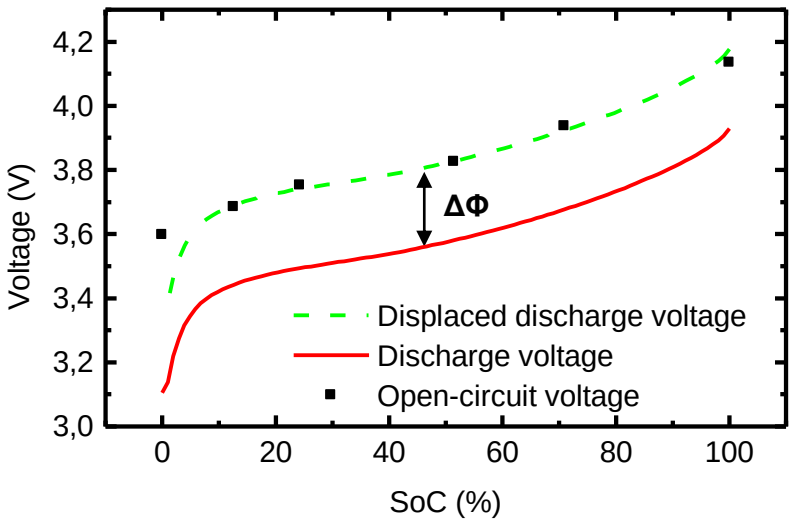

Fig. 3.5. Discharge voltage vs. open-circuit voltage. Dashed line was obtained by shifting the curve of discharge voltage towards V_{OC}

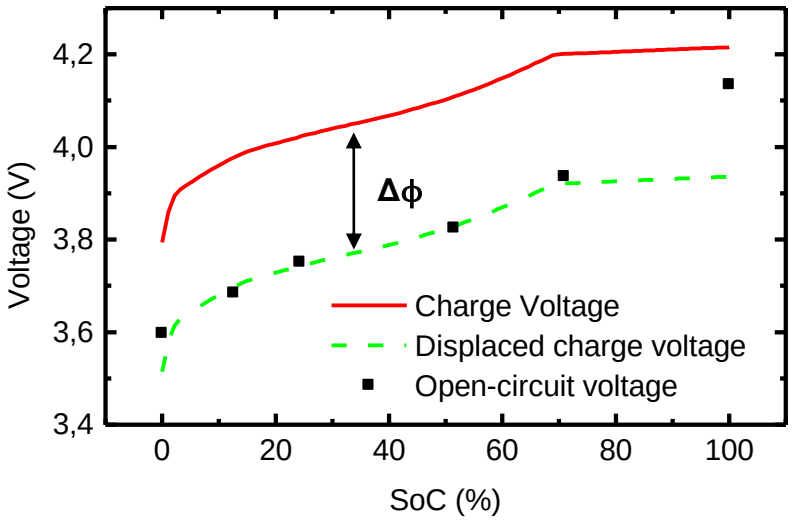

Fig. 3.6. Charge voltage vs. open-circuit voltage. Dashed line was obtained by shifting the curve of charge voltage towards V_{OC}

Table 3.2. Difference between V_{OC} and V_{cell} (Carge rate: 1.00C)

Voltage drop during discharge	Voltage drop during charge
247,38 mV	279,58 mV

Once the overpotential voltage has been obtained, R_η can be calculated (Fig. 3.7). In this case, it is also found to be constant for the whole charge or discharge processes. Cell resistance is constant for the whole process. It is

343mΩ for discharge and 333mΩ for charge. These values agree well with those obtained by the other method (refer to section 3.8). R_η is also higher for discharge than for charge although the difference between them is smaller in that case with respect to *V-I* method.

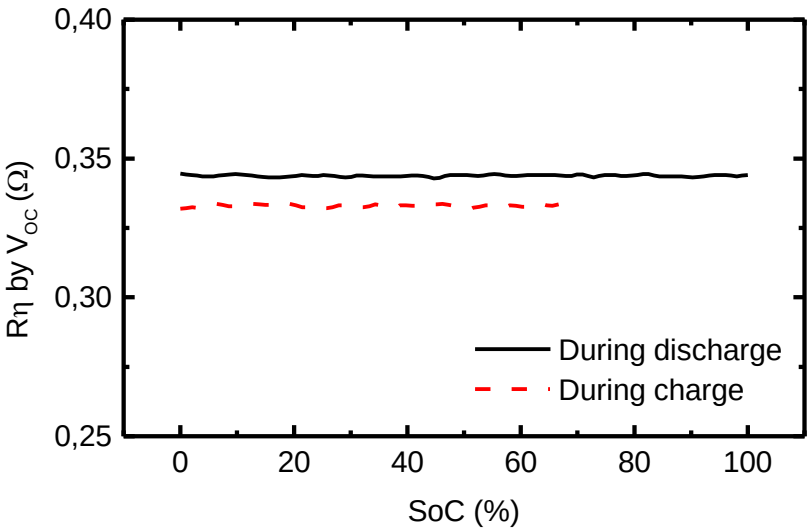

Fig. 3.7. Cell resistance by open-circuit voltage method

3.3.3. dQ_P/dt

Once the cell resistance has been determined, heat generated by overpotential can be estimated from (1.10). As cell resistance was calculated by two different methods, the comparison between two different results is plotted in Fig. 3.8.

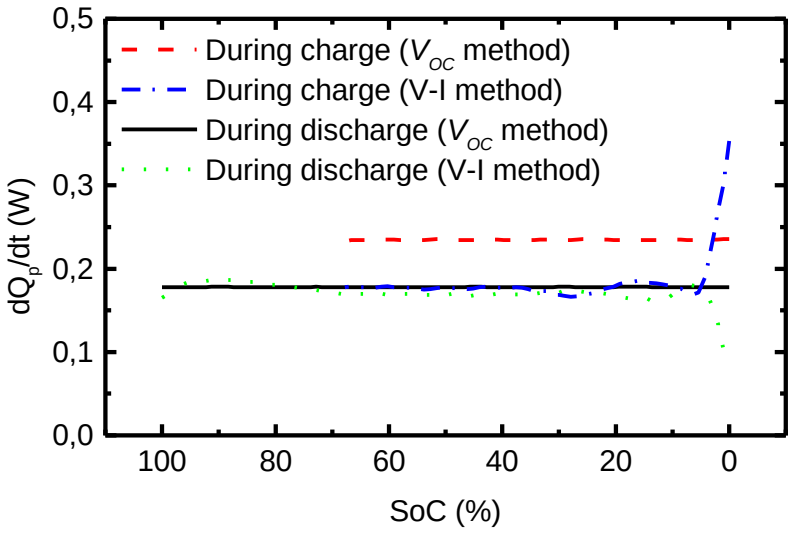

Fig. 3.8. Heat produced by overpotential voltage calculated by different methods

As overpotential resistance and current are constant, it can be seen in Fig. 3.8 that heat produced by overpotential is maintained almost constant regardless of SoC. The heat generated per unit time calculated by V_{OC} method during charge is higher than other results (Table 3.3). This is because overvoltage is higher during charge process than during discharge process (Fig. 3.6). Moreover, values obtained during charge and discharge cannot be compared because current amplitudes while charging and discharging the battery are not the same (as explained in Table 3.1).

Table 3.3. Heat generated per unit time calculated with different methods while charging and discharging the battery

V-I method		V_{OC} method	
Charge	Discharge	Charge	Discharge
178 mW	178 mW	235 mW	178 mW

3.4. Heat produced by the entropy change

A first step to calculate the heat produced by the entropy change is the calculation of the derivative of the open-circuit voltage with respect to the cell temperature (Fig. 3.9) (refer to section 2.3.2.1.). A local maximum around 52 % of the SoC is found, which is coherent with previous works [3] where a minimum value of approximately -1 $mV \cdot K^{-1}$ along with a local maximum in their curves were obtained. However, further measurements would be necessary to exactly determine it.

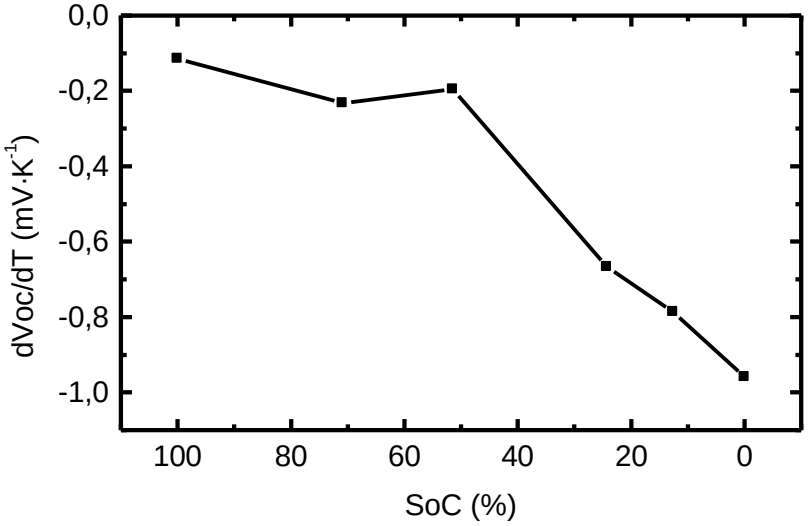

Fig. 3.9. Derivative of Voc with respect to cell temperature for different SoC (100 %, 70.87 %, 51.47 %, 24.27 %, 12.61 % and 0 %)

The entropy change is calculated by multiplying dV_{oc}/dT by the Faraday constant. Larger heat contributions occur in lower SoC (according to (1.9) and (1.11)) as can be seen in Fig. 3.10. Shape and values of ΔS agree well with other studies [19]. They have obtained a minimum value near -70 $J \cdot mol^{-1} \cdot K^{-1}$ and a curve with similar shape.

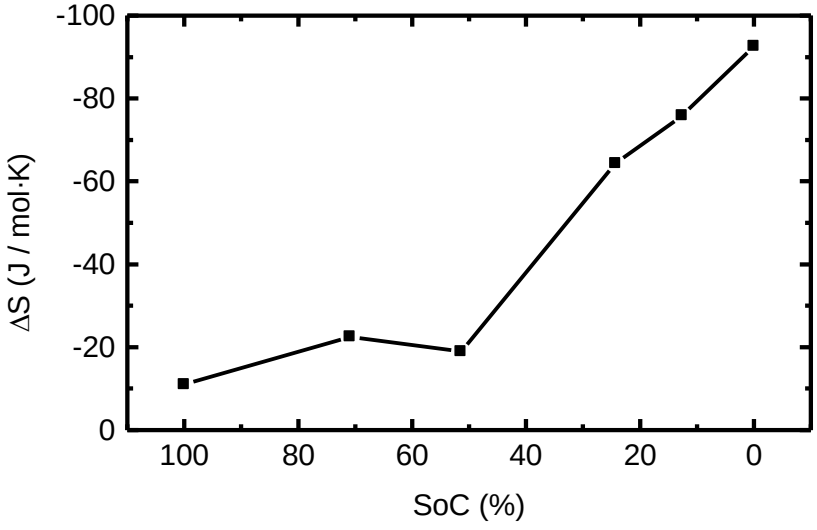

Fig. 3.10. Entropy change depending on SoC

Finally, the heat generated by the entropy change is calculated from the cell temperature, the derivative of the open-circuit voltage with temperature and from the current flowing through the battery. For signs convention, current is considered to be positive during discharge and negative during charge.

Results show that dQ_S/dt is positive during discharge and negative during charge (Fig. 3.11). As this term has a positive contribution in the equation of total heat flow (1.9), it means that during discharge it contributes additional heat while extra energy is generated by cooling the environment during charge (Peltier effect).

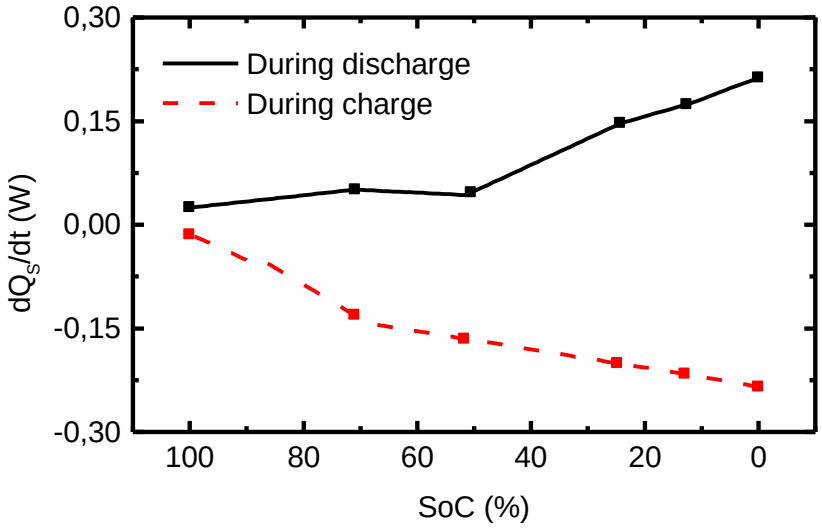

Fig. 3.11. Heat produced by the entropy change (Charge rate: 1.00C)

3.5. Heat Flow

The total heat flow is defined as the contribution of dQ_P/dt and dQ_S/dt according to (1.9). A charge cycle was followed by a discharge cycle to analyze the total heat flow (Fig. 3.12). On the first 50 % SoC during charge, where negative values are obtained; the endothermic nature of the reaction can be seen.

Battery discharge is clearly an exothermic process. The contribution of heat is higher as SoC decreases. It matches well with expected result because also cell temperature rises as end of discharge approximates (Fig. 3.2). Similar curves were obtained in other studies [20].

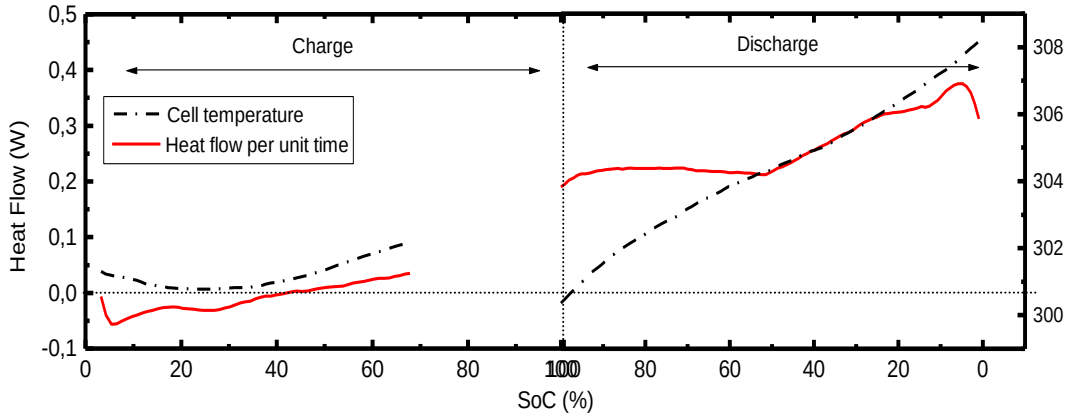

Fig. 3.12. Cell temperature and heat flow in and out of the cell during charge and discharge processes at 1.00C. Where temperature decreases (during charge) it can be seen the endothermic nature of the battery (negative heat flow). During discharge, temperature increases during the whole process giving a positive and increasing heat flow.

Cell temperature variations are related to heat flow. If the battery is being charged or discharged, SoC can be estimated from temperature variations. However, heat flow can be used to calculate an additional variable (like thermal resistance) to estimate the SoH of the battery.

3.5.1. Thermal impedance

The heat behaviour of the battery can be described by a thermal model composed by a capacitor and a thermal resistance (refer to section 1.4.1). They can be obtained by fitting equation (3.5) with the heat flow.

$$\frac{dQ_{Total}/dt}{I^2} = R_t + \frac{t}{C_t} \tag{3.5}$$

During discharge there are two different behaviours in terms of heat flow; there is a first part in which it is maintained almost constant (from 100 % SoC until 52.43 % SoC) and then there is another part in which increases gradually (Fig. 3.12). The first part behaviour could be described by only one contribution: the effect of thermal resistance. Unlike this, on the second part of discharge, there is the contribution of both thermal resistance and capacitor. However, during charge, the curve does not match well with the proposed thermal model (refer to section 1.4). There are negative values and the shape does not correspond either to the behaviour of a capacitance or a resistance.

Thermal resistance and thermal capacitance, while discharging the battery at charge rate of 1.00C, were obtained by fitting the equation to heat flow by Microcal Origin 5.0 (Table 3.4). Obtained values are coherent with previous

studies where thermal resistance values are of some milliohms and capacity values are of some thousands of farads. However, these values were calculated for a NiMH battery [2].

Table 3.4. Thermal resistance and capacity obtained from heat flow during discharge at 1.00C

Thermal resistance	420 mΩ
Thermal capacitor	5045.56 F

Once the heat flow is known, thermal impedance can be calculated using equation (1.14). It is defined as the Fourier transform of heat flow divided by the Fourier transform of the square of current (for further explanation refer to section 1.4.1). Hanning window is used as FFT windowing.

Thermal impedance behaves as a resistance in the considered frequency range because it hardly changes with frequency. Modulus of thermal impedance during discharge and charge is plotted versus frequency in Fig. 3.13 and Fig. 3.14 respectively. We can write:

$$Z_t = Z_p + Z_s \approx R_\eta + R_s \tag{3.6}$$

Where, thermal impedance is represented as the sum of the overpotential resistance R_η and a chemical resistance R_s. This, in fact, is a consequence of the transformation of equation (1.9).

Thermal impedance is founded to be approximately 600 mΩ during discharge and 810 mΩ during charge in those frequencies.

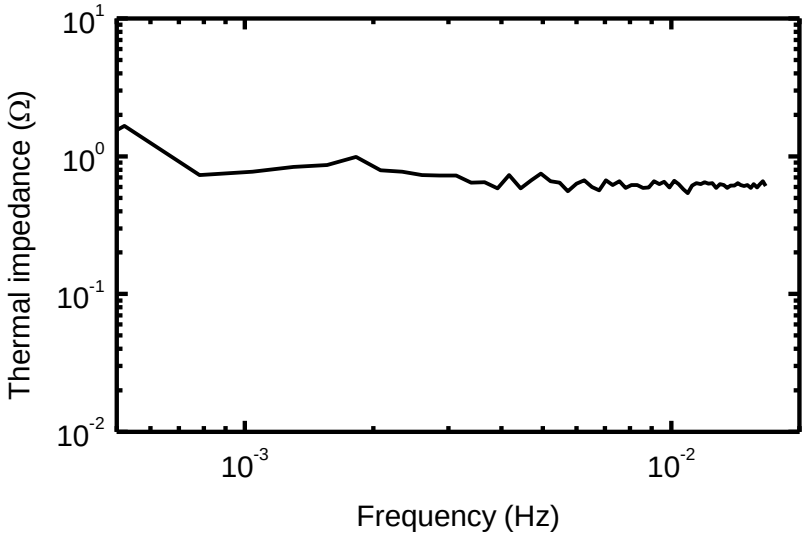

Fig. 3.13. Thermal impedance during discharge (at 1.00C)

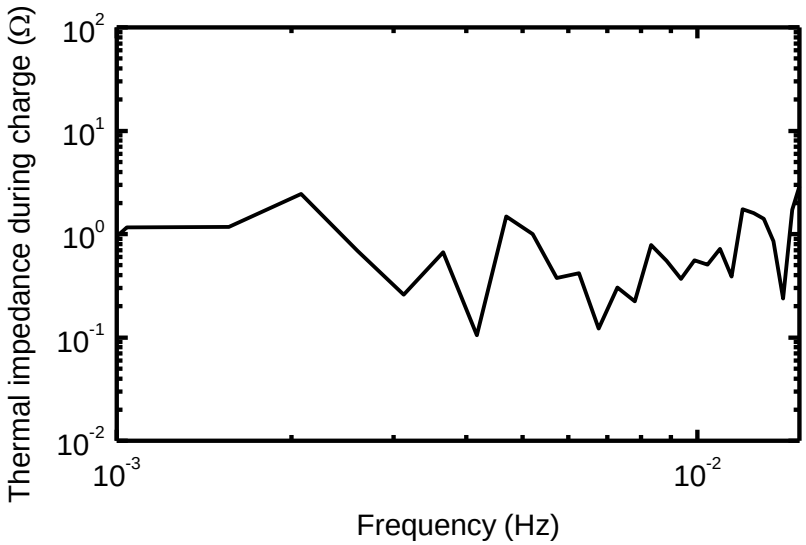

Fig. 3.14. Thermal impedance during charge (at 1.00C)

3.5.1.1 *Comparison with impedance analyzer measurements*

Impedance measurements were carried out with Agilent 4294A (refer to section 2.4 for further details) in order to compare them with obtained results. Thermal impedance and electrical impedance measured by the impedance analyzer are plotted versus frequency (Fig. 3.15). From equation (3.6) we can compare the electrical impedance given by the impedance analyzer (dashed line) with thermal impedance obtained from the thermal analyses (solid line). The difference between them is attributed to the chemical resistance R_s.

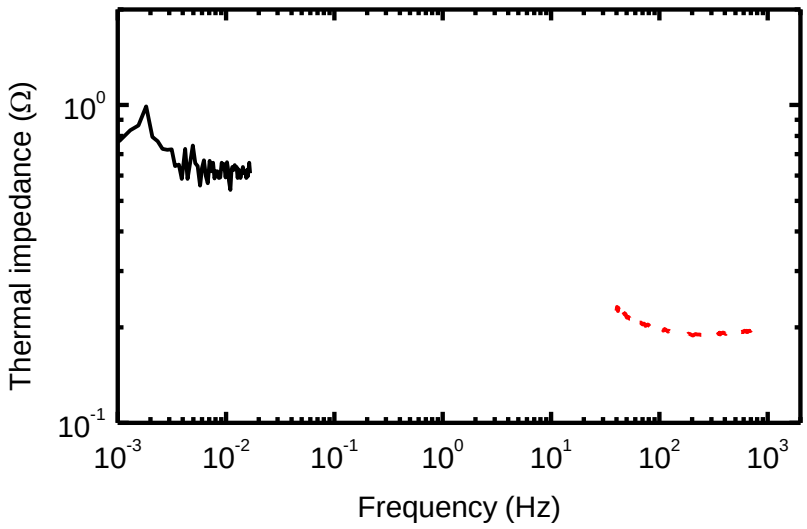

Fig. 3.15. Thermal impedance during discharge at charge rate of 1.00C (in lower frequencies and represented by a solid line) and electrical impedance measured by an impedance analyzer (between 40 Hz and 1 kHz and represented by a dashed line)

3.6. Charge rate dependence

When charging batteries at higher charge rates, dissipated energy increases. This occurs because the minimum acceptable voltage is reached earlier (Fig. 3.16). Also temperature increases to higher temperatures when charging the battery at higher rates. While discharging the battery at 0.50 C the rise of temperature is of 1.74 K while it is of 4.11 K while discharging it at 1.00 C.

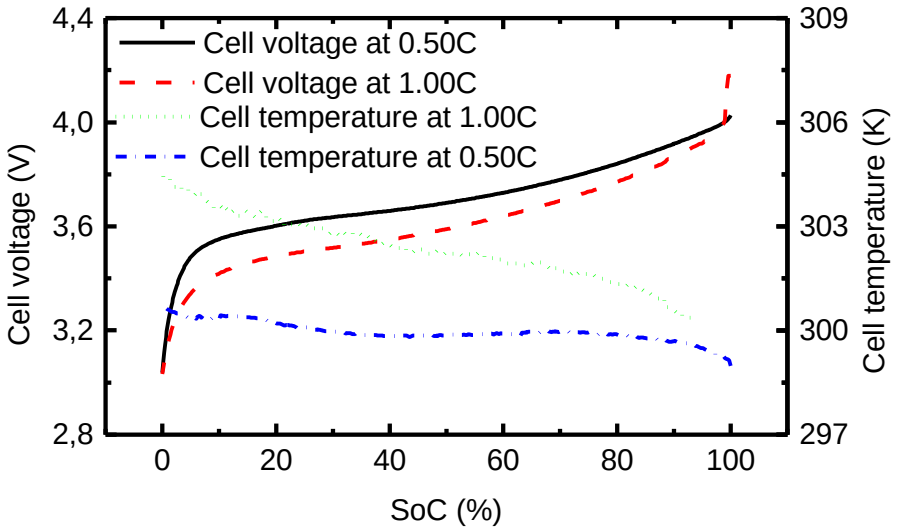

Fig. 3.16. Comparison of cell voltage and cell temperature for charging rates of 1.00C and 0.50C

3.6.1.1 *Heat flow dependence with charge rate*

The heat produced by the Joule Effect does not depend on whether the battery is charged or discharged. However, it depends on the charge rate (Fig. 3.17). As Joule effect is proportional to the square of current, it is smaller as charge rate decreases.

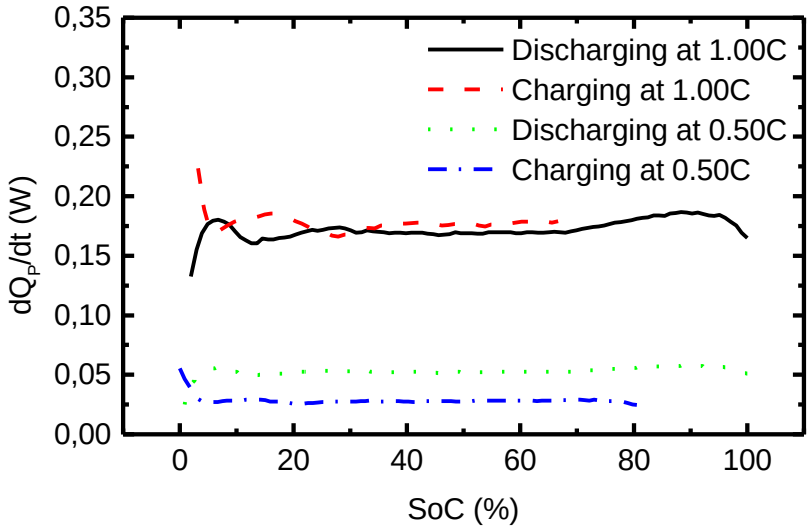

Fig. 3.17. Heat per unit time produced by Joule Effect during charge and discharge at different charge rates (1.00C and 0.50C)

The heat produced by the entropy change depends on whether the battery is being charged or discharged and also on the charge rate. During charge, it is always negative and increases as charge rate decreases. However, during discharge it is always positive and decreases as charge rate decreases (Fig. 3.18). Regardless of the sign, which has been imposed by convention, dQ_S/dt always decreases as charge rate decreases. It is in agreement with expected behaviour because when the battery is charged (or discharged) at lower current during a longer time it becomes less heated. This lower T_{cell} implies then a smaller heat contribution.

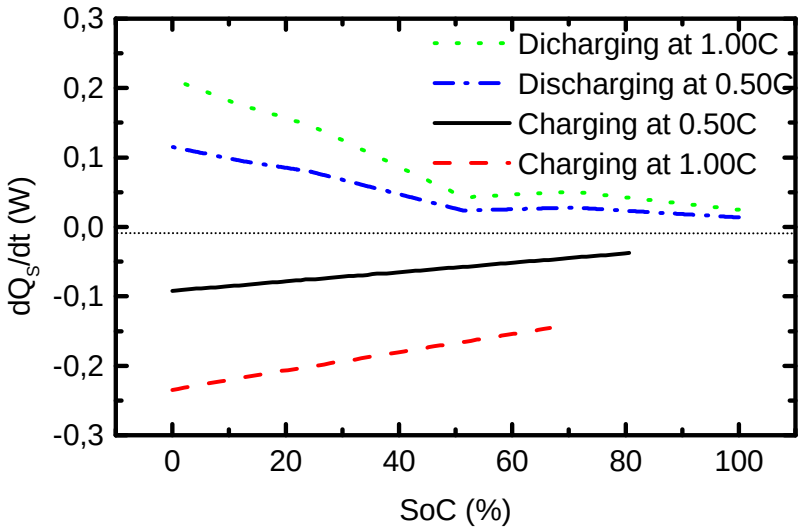

Fig. 3.18. Heat produced by the entropy change while charging and discharging the battery at 1.00C and 0.50C charge rates

Total heat flow during charge and discharge decreases in both cases. For a charge rate of 0.50C, it remains negative until 80 % SoC during charge and it decreases approximately 145 mW (with respect to same result for a charge rate of 1.00 C) during discharge (Fig. 3.19).

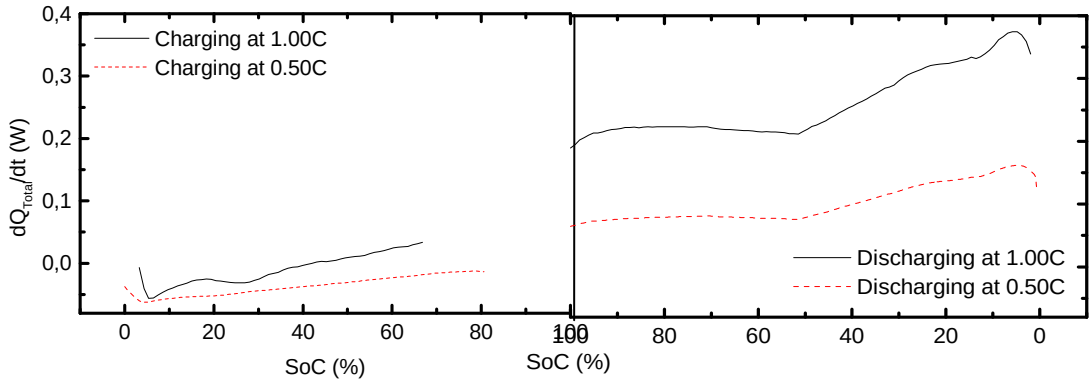

Fig. 3.19. Total heat flow comparison during charge and discharge processes by using different charge rates (0.50C and 1.00C)

3.7. Charge evolution and SoH during cycling

Consecutive cycles (charge plus discharge) were carried out in order to observe how capacity varies. Specifically, 27 cycles were monitored (Fig. 3.20). Injected and extracted charges were calculated for every cycle (Fig. 3.21) by integrating in time the current delivered to or drawn from the battery. Extracted charge is almost constant while injected charge tends to decrease.

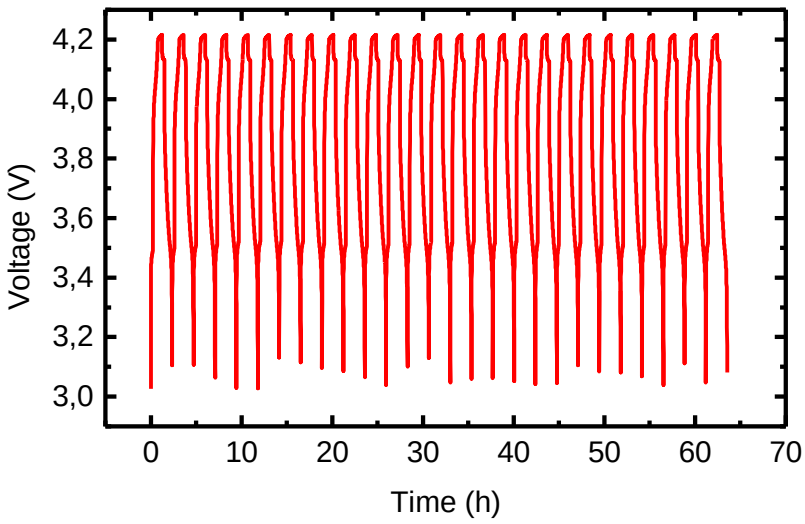

Fig. 3.20. Cell voltage evolution during consecutive cycles

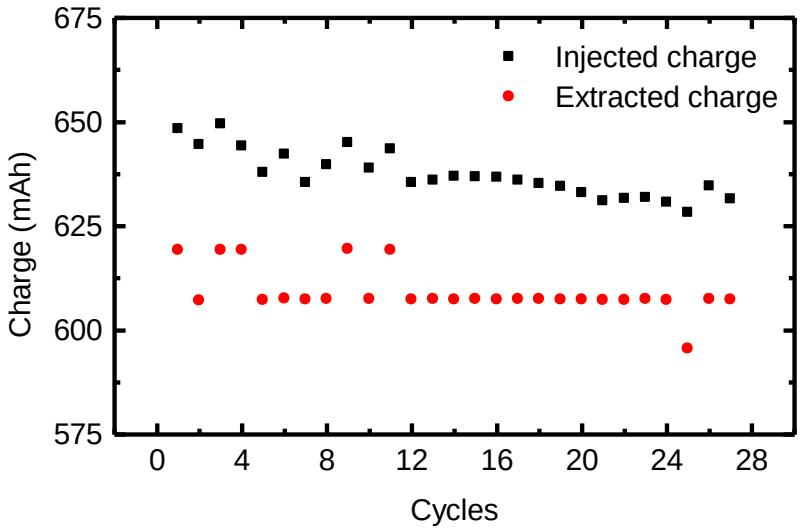

Fig. 3.21. Injected and extracted charges measured by integrating the current in time for different successive cycles.

The decrease of injected charge could be associated to the fact that battery capacity is diminishing. It would mean that SoH is worsening and thus, it could be estimated from the integrated charge (Fig. 3.22). As can be observed, SoH tends to decrease as number of cycles increases; it starts near 88 % SoH and finishes near 85 % SoH in the studied range.

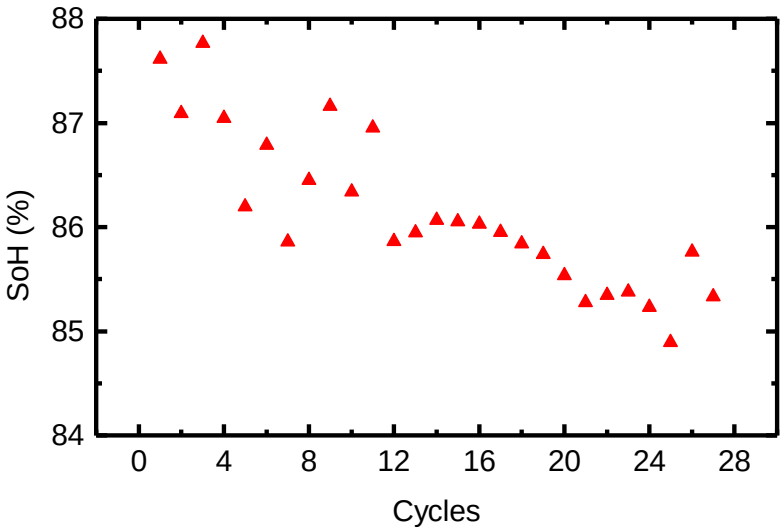

Fig. 3.22. SoH evolution for consecutive cycles

3.8. Comparison of resistance obtained by different methods

Cell resistance and thermal resistance are calculated by different methods as illustrated in Table 3.5. The difference between *V-I* characteristics and V_{OC} method is the way in which overpotential resistance is calculated (for further information refer to section 3.3). DC OhmTests method is that used by Cadex equipment (as described in section 2.2.1). And, finally, thermal resistance is obtained from literature [2] and it considers the heat flow of the battery. Thermal resistance obtained through heat flow is obtained by fitting equation (3.5) to the total heat flow during discharge process. However, thermal resistance through Fourier transform is obtained by equation (1.14). Thermal resistance is not calculated for charge process. It is because heat flow during charge has negative values and it behaves neither as a resistor nor as a capacitance (Fig. 3.12). It can be concluded that during charge, thermal model purposed in section 1.4.1 is not working for thermal behaviour of lithium-based batteries that are being charged.

Table 3.5. Resistance obtained by different methods during charge and discharge processes

Method	Resistance during charge (mΩ)	Resistance during discharge (mΩ)
V-I characteristics	250	330
V_{OC} method	333	343
By DC OhmTest method from Cadex	-	245
Thermal resistance through heat flow (charge rate: 1.00C)	Proposed model is not well-adjusted to results	420
Thermal resistance through Fourier transform (charge rate: 1.00C)	Proposed model is not well-adjusted to results	600

CHAPTER 4. CONCLUSIONS

In this thesis, we monitored current, voltage and temperature profiles for several charge/discharge cycles in order to propose a model to determine the SoC and SoH of the battery from its thermal behaviour. Temperature was measured directly with the thermistor present in Li-ion batteries. From these measurements we inferred the electrical resistance and thermal impedance from an accurate determination of heat flows in the battery. Finally, we found a relationship between thermal fluctuations, heat flow and the SoC and SoH of the battery.

Resistance values obtained through two different methods (*V-I* characteristics and V_{OC} method) are consistent with expected. Values obtained by both methods during discharge almost coincide while during charge they are smaller (especially when using *V-I* method). In a portable solution, it would be preferable *V-I* characteristics method in front of V_{OC} method. It is mainly because V_{OC} does not need to be measured or calculated when employing this method. V_{OC} depends on many parameters and it is difficult to measure. With this method, only two currents should be injected and cell voltage measurements should be done for every one of these currents. SoC cannot be estimated by only knowing resistance variations (it hardly varies with SoC). However, resistance increases as SoH decreases.

Heat generated by Joule effect does not depend on the process of charge or discharge. It basically depends on charge rate; it increases as heat rate increases. This was expected because as current increases, more heat is dissipated by this effect.

Charge process is found to be endothermic while discharge process is exothermic. Cell temperature variations are higher when discharging the battery. This results in a positive contribution of heat generated by the entropy change to heat flow during discharge and negative during charge. Total heat flow during charge at 0.50C and 1.00C charge rates has negative values.

Regarding to the main objective, it was observed that SoC can be estimated through the heat flow of the battery. Temperature measurements, taking advantage of thermistor already present in lithium-based batteries, are essential for this estimation. This is a significant contribution because thermal battery monitoring had been performed in non-portable calorimeters. Yet, we have proposed a new definition for both SoC and SoH to consider their relationship.

The thermal model proposed by Xiao et al. [2] has been successfully introduced to adjust the thermal behaviour of Li-ion battery during discharge. We obtained a thermal resistor in series with a thermal capacitance. Their magnitudes have been estimated by fitting thermal equations to the heat flow curve during discharge.

SoH was estimated for consecutive cycles. It was observed that it has a tendency to decrease with cycles, as expected.

All results obtained in this study should be extended to a general case. This issue requires more measurements to finally obtain an low power electronic system able to determine the SoC and SoH:

- Room temperature should be considered as battery behaviour depends on it.
- A more precise determination of the open-circuit voltage as function of the SoC should be of interest.
- Different charge rates should be considered. Also pulsed discharge that describes better real situations should be tested.
- Different battery capacities.
- Measurements with different Li-ion battery models.
- Tests with different types of Li-ion batteries, as Li-Po batteries, would be interesting.

In conclusion, batteries are very complex systems and their behaviour depends on many parameters: each battery is different and its performance depends also on how it is used. Thus, a more complete study on the investigated parameters (electrical and thermal impedances) on temperature, SoC and SoH are necessary.

BIBILIOGRAPHY

[1] Onda, K., Kameyama, H., Hanamoto, T. and Ito, K., "Experimental Study on Heat Generation Behavior of Small Lithium-Ion Secondary Batteries", *Journal of the Electrochemical Society*, 150 (3), A285-A291 (2003)

[2] Xiao, P., Gao, W., Qiu, X., Zhu, W., Sun, J. and Chen, L., "Thermal behaviors of Ni-MH batteries using a novel impedance spectroscopy", *Journal of Power Sources*, 182, 377-382 (2008)

[3] Takano, K., Saito, Y., Kanari, K., Nozaki, K., Kato, K., Negishi, A. and Kato, T., "Entropy change in lithium ion cells on charge and discharge", *Journal of Applied Electrochemistry*, 32, 251-258 (2002).

[4] Kiehne, H.A., "*Battery Technology Handbook*", Marcel Dekker, Remmingen-Malsheim (2003)

[5] Cuadras, A., Tröltzsch, U. and Kanoun, O., "Low energy battery monitoring", *Eurosensors XXII*, S. 1490-1493 (2008)

[6] Batteries in a portable world (from Cadex)
http://www.buchmann.ca/chap6-page1.asp
Last accessed 02nd November of 2010

[7] Snihir, I., Rey, W., Verbitskiy, E., Belfadhel-Ayeb, A. and Notten, P. H. L., "Battery open-circuit voltage estimation by a method of statistical analysis", *Journal of Power Sources*, 159 (2), 1484-1487 (2006)

[8] Patrick K. NG and Like Xie, "Lithium ion battery for telecommunications applications", *proceedings of the Battcon conference* (2004)

[9] Battery University (sponsored by Cadex Electronics Inc.)
Buchmann, Isidor. (2006). *The high-power lithium-ion*
Available: http://www.batteryuniversity.com/partone-5A.htm
Last accessed 07th October of 2010

[10] Mpoweruk
http://www.mpoweruk.com/performance.htm
Last accessed 02nd November of 2010

[11] Huggins, R.A., "General equivalent circuit of batteries and fuel cells", *Technische Fakultät, Christian.Albrechts-Universität*, Germany.

[12] Vogel, C., "Build Your Own Electric Motorcycle", McGraw Hill Professional (2009)

[13] Cadex Electronics Inc.
Available: http://www.cadex.com/
Last accessed 07th October of 2010

[14] Varta Microbattery
LIP 533048 AJ datasheet (2008)
Available:http://www.varta-microbattery.com/en/mb_data/documents/data_sheets/DS56466.pdf
Last accessed 07th October of 2010

[15] Agilent Technologies
Available: www.agilent.com
Last accessed 07th October of 2010

[16] Tektronix
Available:
http://www2.tek.com/cmswpt/psdetails.lotr?ct=PS&cs=psu&ci=13540&lc=EN
Last accessed 07th October of 2010

[17] Ovan
Available: www.ovan.es
Last accessed 07th October of 2010

[18] *Agilent Impedance Measurement Handbook*
Available: http://cp.literature.agilent.com/litweb/pdf/5950-3000.pdf
Last accessed 07th October of 2010

[19] Okamoto, E., Nakamura, M., Akasaka, Y., Inoue, Y., Abe, Y., Chinzei, T., Saito, I., Isoyama, T., Mochizuki, S., Imachi, K. and Mitamura, Y., "Analysis of heat generation of lithium ion rechargeable batteries used in implantable battery systems for driving undulation pump ventricular assist device", *Artifical Organs*, 31(7), 538-541 (2007)

[20] Gunderson, D., "Li-ion battery temperature trends during charge and discharge"
Available: http://www.micro-power.com/userfiles/file/mp_tempcharge-1250026530.pdf
Last accessed 10th November of 2010

ANNEX

Preliminary Data Sheet [1]

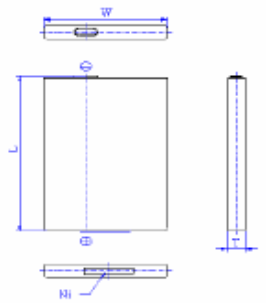

Type Designation Type Number	LIP 533048 AJ 56466
System	Li-Ion
UL Recognition	UL 1642 (pending)
Nominal Voltage [V] Typical Capacity [mAh] Minimum Capacity C [mAh]	3.7 (average) 740 (at C/5 from 4.2 V to 2.75 V at 20°C) 700 (at C/5 from 4.2 V to 2.75 V at 20°C)
Dimensions [mm] Width (w) Thickness (t) Height (L)	 30.0 +0/-0.6 5.3 Max 47.8 +0/-0.6
Weight, approx. [g]	17
Charging Method Charge Voltage [V] Initial Charge Current [mA]	Constant Current + Constant Voltage 4.20 (+/- 50 mV) Standard Charge: 350 Rapid Charge: 700
Charging Cut-Off (a) or b)) a) by time [h]	 Standard Charge: 3 Rapid Charge: 2.5
b) by min. current [mA]	C/50
Discharge Cut-Off voltage [V]	3.0
Max. Continuous Discharge Current [mA]	1400
Operating Temperature [°C]	Charge: 0 to 45 Discharge: -20 to 45
Storage Temperature [1)]	1 Year at -20 to +25°C 3 Month at -20 to +45°C 1 Month at -20 to +60°C
Impedance Initial [mΩ]	< 60 @ 1kHz
Life Expectancy 20°C [Cycles]	300 cycles 1C/1C ≥80 % of rated discharge capacity

[1]) Storage at initial cell voltage of 3.8 to 4.0 V/cell.